Understanding *Plasmodium vivax* recurrent infections using an amplicon deep sequencing assay, PvAmpSeq, identity-by-descent and model-based classification

Authors and Affiliations

Jason Rosado[1,2]*, Jiru Han[3,4], Thomas Obadia[1,5], Jacob Munro[3,4], Zeinabou Traore[1], Kael Schoffer[4], Jessica Brewster[4], Caitlin Bourke[4], Joseph M. Vinetz[6,7], Aimee R. Taylor[1], Michael White[1], Melanie Bahlo[3,4], Dionicia Gamboa[7,8,9], Ivo Mueller[1,4,10ɣ], Shazia Ruybal-Pesántez[4,10,11*ɣ^]

1. Institut Pasteur, Université Paris Cité, Infectious Diseases Epidemiology and Analytics G5 Unit, Institut Pasteur, Paris, France
2. Université Paris Cité, Institut de Recherche pour le Développement, MERIT, Paris, France
3. Genetics and Gene Regulation Division, Walter and Eliza Hall Institute of Medical Research, Melbourne, Australia
4. Infection and Global Health Division, Walter and Eliza Hall Institute of Medical Research, Melbourne, Australia
5. Institut Pasteur, Université Paris Cité, Bioinformatics and Biostatistics Hub, Institut Pasteur, Paris, France
6. Section of Infectious Diseases, Department of Internal Medicine, Yale School of Medicine, New Haven, CT, USA
7. Instituto de Medicina Tropical Alexander von Humboldt, Universidad Peruana Cayetano Heredia, Lima, Peru
8. Laboratorio de Malaria, Laboratorios de Investigación y Desarrollo, Facultad de Ciencias e Ingeniería, Universidad Peruana Cayetano Heredia, Lima, Peru
9. Departamento de Ciencias Celulares y Moleculares, Facultad de Ciencias e Ingeniería, Universidad Peruana Cayetano Heredia, Lima, Peru
10. Department of Medical Biology, School of Medicine and Health Sciences, University of Melbourne, Melbourne, Australia
11. Vector-borne Diseases and Tropical Public Health, Burnet Institute, Melbourne, Australia

***Correspondence**

E-mail: jjrosados@gmail.com; s.ruybal@imperial.ac.uk

ɣ: Co-senior authors contributed equally to this work.
^ Current affiliations: MRC Centre for Global Infectious Disease Analysis, School of Public Health, Imperial College London, London, UK, and Institute of Microbiology, Universidad San Francisco de Quito, Quito, Ecuador

Summary

Plasmodium vivax infections are characterised by recurrent bouts of blood-stage parasitaemia. Understanding the genetic relatedness of recurrences can help distinguish whether these are caused by relapse, reinfection, or recrudescence, which is critical to understand treatment efficacy and transmission dynamics. We developed PvAmpseq, an amplicon sequencing assay targeting 11 SNP-rich regions of the *P. vivax* genome. PvAmpSeq was applied to field isolates from a clinical trial in the Solomon Islands and a longitudinal observational cohort in Peru, and statistical models were applied for genetic classification of recurrences. In the Solomon Islands trial, where participants received antimalarials at baseline, half of the recurrent infections were caused by parasites with >50% relatedness to the baseline infection (identity-by-descent), with statistical models providing further classification as probable relapses and recrudescences, although with wide uncertainty. In the Peruvian cohort, half of the recurrent infections were caused by parasites with >22% relatedness to the baseline infection. PvAmpSeq provides high-resolution genotyping to characterise *P. vivax* recurrences, offering insights into transmission and treatment outcomes. We also discuss the nuances and limitations of available statistical methods for the classification of *P. vivax* genotyping data.

Keywords: *Plasmodium vivax*, recurrences, relapses, microhaplotypes, genetic diversity

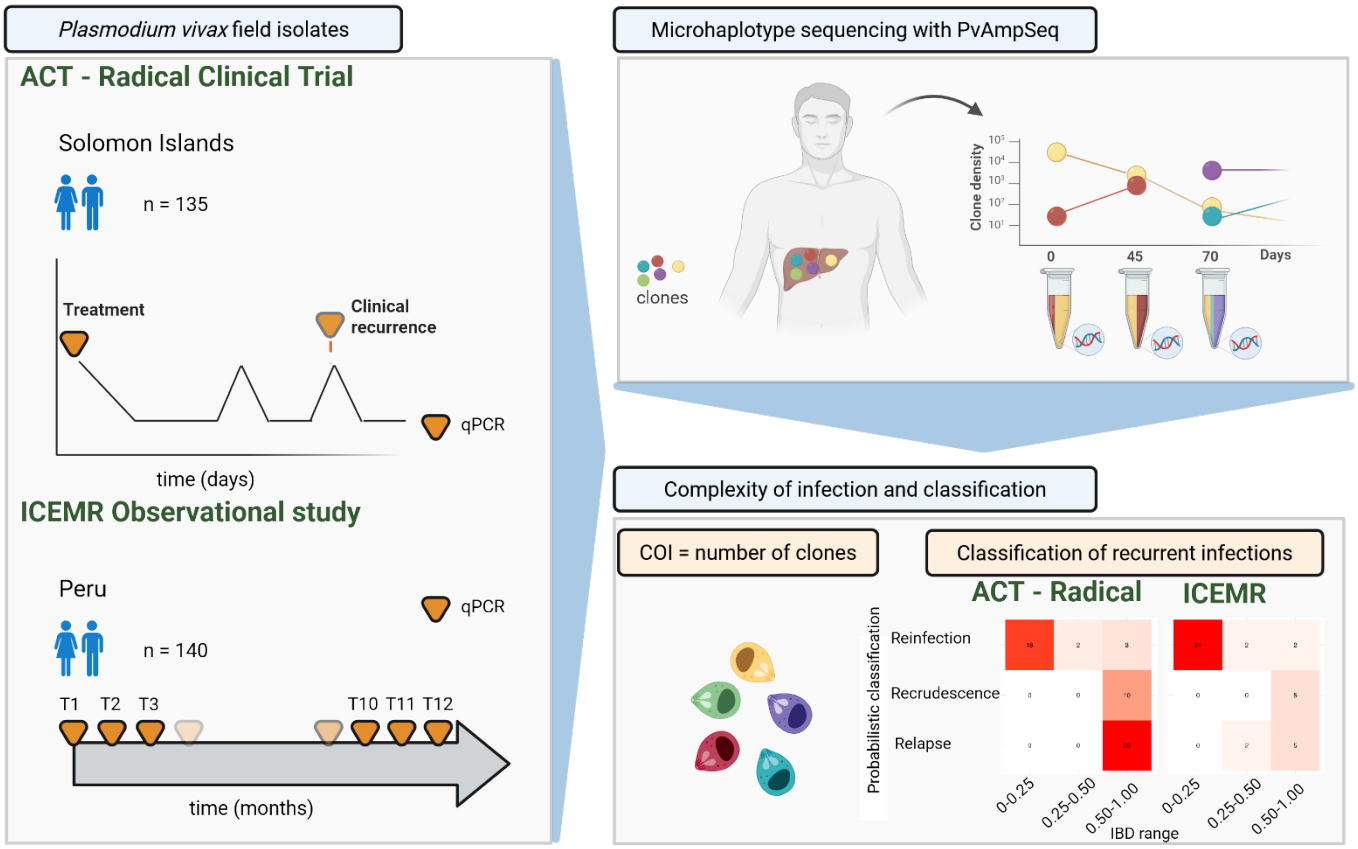

Graphical abstract. Created in BioRender. Rosado, J. (2026) https://BioRender.com/p66i686

83 # Introduction

84 *Plasmodium vivax* is the most widespread *Plasmodium* parasite infecting humans, causing an estimated 9.2 million
85 malaria cases per year.[1] The ability of *P. vivax* to remain in the liver as dormant hypnozoites and to cause subsequent
86 (and often multiple) blood-stage infections contributes to onward transmission and impedes efforts to eliminate
87 malaria.[2] In areas endemic for *P. vivax,* recurrent *P. vivax* infections can result from relapses but also recrudescence
88 (due to antimalarial treatment failure if the individual received treatment) or reinfections (from a new mosquito bite).
89 Distinguishing between relapses, recrudescences, and reinfections is crucial for the assessment of the effectiveness of
90 antimalarial-based control strategies and understanding *P. vivax* biology and epidemiology, but remains a major
91 challenge.

92 The WHO Global Malaria Programme has recently highlighted the importance of using more sensitive, easily
93 implemented, and reproducible tools that allow for estimating the efficacy of clinical drug trials.[3] Comparing parasite
94 genotypes of baseline infections with the ones from recurrent infections allows us to better estimate drug failure rates
95 through 'molecular correction' broadly based on the identification of the same, closely related, or distinct genotypes.
96 Unlike *P. falciparum* malaria, where genotyping must distinguish between recrudescences and reinfections, genotype
97 data from *P. vivax* recurrent infections must be able to discriminate reinfections from both recrudescences and
98 relapses for evaluation of treatment efficacy. Classically, genotyping infections for 'molecular correction' in drug-
99 efficacy clinical trials has been done with length-polymorphic genetic markers,[4] but more recently with amplicon
100 sequencing approaches.[3,5,6] A limitation of length-polymorphic genotyping can be the insufficient resolution to detect
101 minority clones in infections.[7] This can result in an overestimation of treatment efficacy in clinical trials. Undetected
102 parasite clones could represent drug-resistant parasites, recrudescent clones, or hypnozoite-derived parasites, which
103 were not detected at baseline.

104 The sequencing of Single Nucleotide Polymorphism (SNP) or SNP-rich amplicons by next-generation sequencing
105 approaches (Amplicon deep sequencing or AmpSeq) has been shown to overcome the drawbacks of microsatellites.[8]
106 For example, i) detection of multiple SNPs in the same read allows direct detection of haplotypes, ii) sufficient
107 sensitivity to detect minor clones and track marker-wise clone dynamics over time in *Plasmodium* infections,[7,9–11] and
108 iii) high reproducibility. For *P. falciparum,* AmpSeq genotyping has been shown to improve the classification of
109 recrudescences and reinfections in clinical trials.[5,12]

110 In addition to their use for evaluation of treatment efficacy, AmpSeq markers are also being used to identify imported
111 malaria cases,[13] estimate transmission levels in population studies,[14] detect drug-resistant parasites,[14–19] and
112 characterise *Plasmodium* population genetics[18,20–25]. In addition, *P. vivax* genome-wide panels of AmpSeq markers and
113 Molecular Inversion Probes (MIPs) have recently been developed for population genetics, geographic origin
114 assignment, and detection of SNPs associated with drug resistance (see comparative Table S1).[6,18,26–30] In a recent study
115 by Kleinecke and colleagues, a panel of 93 genome-wide AmpSeq microhaplotypes was applied in a clinical trial to
116 classify 108 primary and recurrent infection pairs using identity-by-descent (IBD) estimates.[6] The study showed a
117 higher frequency of suspected relapses or recrudescences (high IBD) (84%) in patients not treated with primaquine
118 (PQ) compared to those with PQ (60%).

119 To advance our understanding of *P. vivax* recurrent infections, we developed a *P. vivax* AmpSeq (PvAmpSeq) assay
120 that targets 11 highly polymorphic SNP-rich regions or microhaplotypes (across 11 chromosomes) and applied several
121 recently developed approaches for studying infections at the clone level using IBD and probabilistic models. Here, we
122 show the application of PvAmpSeq for two cases: on samples from a clinical trial where genetic classification of
123 recurrent infections is necessary for molecular correction of drug failure rates and from a community cohort where
124 genetic classification is useful to understand *P. vivax* epidemiology and transmission patterns. We used samples from
125 the artemisinin- combination therapies (ACT)-Radical randomised-controlled clinical trial conducted in the Solomon
126 Islands between 2018 and 2019, involving patients receiving three different drug combinations, with the overall aim
127 to test for potential antagonistic effects of the drug combinations.[31] Two of the trial arms included drug combinations
128 involving the anti-hypnozoite antimalarial drug PQ, where patients were treated to clear both blood-stage parasites
129 and hypnozoites at baseline. We also used samples from an observational longitudinal cohort in the Loreto region of
130 the Peruvian Amazon, where individuals were followed up between December 2014 and December 2015.[32] We
131 processed PvAmpSeq sequencing data using the AmpSeqR R package to demultiplex and analyse AmpSeq data[33] and
132 used various approaches for genetic classification of recurrent infections. Overall, our findings point to the potential
133 for PvAmpSeq to provide important insights about recurrent infection dynamics in both clinical trials and
134 epidemiological studies.

135

136

137

STAR Methods

Experimental Model and Subject Details

Ethics

Ethical approval for the Solomon Islands ACT-Radical clinical trial was obtained from the Solomon Islands Health Research and Ethics Review Board (HRE 041-16) and the Walter and Eliza Hall Institute of Medical Research Human Research Ethics Committee (WEHI 16-08). The Peruvian cohort study was approved by the Institutional Ethics Committee at the Universidad Peruana Cayetano Heredia (UPCH) (SIDISI 57395/2013) and by the University of California San Diego Human Subjects Protection Program (Project # 100765). UPCH also approved the use of the *P. vivax* DNA samples at the Institut Pasteur (SIDISI 100873/2017).

Study sites and samples

Samples from the Solomon Islands were collected as part of the ACT-Radical clinical trial (registered under Australia and New Zealand Clinical Trials Registry ANZCTR 12617000329369) conducted between September 2017 and February 2019. Briefly, 374 individuals were enrolled in the study of whom 82% (307/374) of participants had a primary symptomatic *P. vivax* infection confirmed by qPCR and were treated with artemether-lumefantrine (AL), AL plus primaquine (AL+PQ), or dihydroartemisinin-piperaquine plus primaquine (DP+PQ). Of these, 307 individuals were actively followed for up to 168 days or until a recurrent *P. vivax* infection was confirmed by light microscopy. qPCR was performed after study completion on stored samples. 191 individuals had *P. vivax* recurrent infections confirmed by light microscopy or qPCR. Of the positive blood samples, 218 (from 91 participants) were available for PvAmpseq evaluation. Blood samples were collected in EDTA tubes for the baseline infections (n = 91), whereas recurrent infection samples were collected as dried blood spots (DBS) (n = 137).

Details on the Peruvian cohort have been previously reported.[32,34] Briefly, a three-year-long observational cohort study was conducted in Peru from December 2012 to December 2015 in two Amazonian villages in the Loreto Region: San José de Lupuna and Cahuide as part of the Amazonian International Centre of Excellence in Malaria Research (ICEMR) study.[34] Using home-to-home and community-based screening, volunteers ≥ 3 years old were invited to be part of this cohort. Between December 2014 and December 2015, participants were monthly sampled, and 1083 out of 7612 blood samples (14.2%) were positive for *P. vivax* by qPCR. Of these positive samples, 449 DNA *P. vivax* positive samples (from 176 participants) were available at Institut Pasteur for genomic studies. As these samples were originally diagnosed by SYBR Green-based qPCR methods and most of them had low parasite density infections (1.55 parasites/µL [IQR: 0.74–8.38]),[32] we performed a diagnostic Taqman qPCR to downselect amplifiable samples. This

167 selection resulted in 274 DNA samples from 152 participants with at least 1 qPCR positive result for *P. vivax* in the last
168 12 months of follow-up (1 *P. vivax* infection = 65 participants, 2 *P. vivax* infections = 56 participants, 3 *P. vivax* infections
169 = 24 participants, 4 *P. vivax* infections = 6 participants).
170 All cohort participants provided written informed consent for participation in both studies. Parental written consent
171 and assent were obtained in the case of participants <18 years in the Peruvian cohort.

172 Method Details

173 **DNA extraction and qPCR**

174 In the Solomon Islands ACT-Radical clinical trial, whole-blood samples from participants at baseline were collected in
175 EDTA tubes and conserved at -20°C until DNA extraction. Genomic DNA was extracted from 200 µL of whole blood
176 using the Favorprep 96-well genomic DNA kit (Favorgen, cat # FADWE 96004, Taiwan) and following the
177 manufacturer's recommendations. PBS buffer was added to the samples with insufficient volume (< 200 µL). Dried
178 blood spots (DBS) from participants with recurrent infections were collected onto filter paper and left to dry at room
179 temperature. DBS samples were conserved at -20°C until DNA extraction. DBS samples were cut into 6mm diameter
180 bloodspot discs using a hole punch. Five bloodspot discs per sample were utilised for DNA extraction using the
181 Favorprep 96-well genomic DNA kit. Genomic DNA from whole blood and DBS was eluted in 50 µL of elution buffer
182 and stored in 96-well plates at -30°C until their use.
183 In the Peruvian cohort, blood samples were collected by finger prick onto filter paper and left to dry at room
184 temperature. DNA was isolated from DBS using the E.Z.N.A. Blood DNA Mini Kit (Omega Bio-tek, Inc., Norcross, GA,
185 US), and molecular diagnosis was performed using the Mangold method.[35,36]
186 For parasite density quantification, we performed a duplex TaqMan qPCR assay combining specific primers and probes
187 targeting the *18s rRNA* gene region of *P. falciparum* and *P. vivax* in a duplex reaction, as reported by Rosanas-Urgell
188 *et al*., with slight modifications.[37] The reaction was prepared in a total of 13 µL containing 1X GoTaq® Probe qPCR
189 Master Mix (Promega, USA), 769 nM of forward and reverse primers, 384 nM of probe, 1.5 µL of Nuclease-free water,
190 and 2 µL of DNA sample. The PCR conditions consisted of an initial denaturation at 95 °C for 2 min, followed by
191 amplification for 45 cycles of 15 s at 95 °C and 1 min at 58 °C. The assay was run in a QuantStudio TM 5 Real-Time PCR
192 system (Applied Biosystems, USA). The number of copies of 18s rRNA DNA/µL of DNA was determined by using a
193 standard curve from a sevenfold serial dilution to 1:10 of a plasmid at concentrations of 1×10^5 copies/µL down to 1
194 copy/µL in nuclease-free water. Samples with late amplification (Cq value >40 & <44; <1 copy/µL) were confirmed by

195 an extra run. *P. falciparum* and *P. vivax* primers and probes detect 3 copies of 18s rRNA DNA per genome. This implies
196 that a concentration of 5 copies/µL in a sample is equivalent to approximately 1-2 parasites/µL.

197 **Marker selection and primer design**

198 A panel of highly informative amplicons was designed, based on whole genome sequencing (WGS) data publicly
199 available from the MalariaGEN *Plasmodium vivax* Genome Variation version 1.0 (PvGV) Project, accessed in June
200 2018.[38] Briefly, FASTQ files were downloaded from the SRA, and SNP/indel variant calling was performed according to
201 GATK V4 best practices against the PvP01 reference genome. Of the 354 WGS samples processed, 154 were excluded
202 due to low coverage (< 5x median coverage), high SNP missingness (>10%), multi-clonality checks (Fws < 0.85) or being
203 from a country with too few samples remaining (n < 15; Vietnam, n = 10; Myanmar, n = 7; Malaysia, n = 6; Indonesia,
204 n = 4; Brazil, n = 2; Laos, n = 2; China, n = 1; India, n = 1; Madagascar, n = 1; and Sri Lanka, n = 1), leaving 203 WGS
205 samples from 6 countries (Thailand, n = 85; Cambodia, n = 31; Peru, n = 28; Colombia, n = 25; Mexico, n = 18; and
206 Papua New Guinea, n = 16). Genomic regions were then excluded based on the coverage distribution across remaining
207 samples as follows: the genome was divided into 1000 bp bins, and coverage was assessed with samtools bedcov[39] for
208 both high mapping quality (HMQ, mapping quality >= 30) and low mapping quality (LMQ, mapQ <= 30) reads. Coverage
209 was then normalised within samples by dividing by the sample median HMQ coverage. Genomic regions were then
210 excluded if the median across samples was greater than 1.5 or less than 0.5 or if the median proportion of HMQ
211 coverage was less than 0.5. This method resulted in the exclusion of the majority of the hypervariable sub-telomeric
212 regions of PvP01. The remaining genome was then searched for all regions that contained at least 4 SNPs within 140
213 bp, with primer design attempted using Primer3[40] with an optimal length of 22 bp and optimal melting temperature
214 of 60 °C, avoiding SNPs and indels in the primer region.

215 **PvAmpSeq assay**

216 The PvAmpSeq assay amplifies 11 SNP-rich regions, or microhaplotype markers, located across 11 chromosomes.
217 Detailed protocols are described in https://doi.org/10.5281/zenodo.17474689. Briefly, PvAmpSeq libraries were
218 prepared after amplification using a nested PCR strategy. Due to the low parasitaemia of *P. vivax* infections frequently
219 found in field samples, parasite genomic regions encompassing marker-specific sites were enriched by multiplex
220 primary PCRs (pPCR) with 25 cycles of amplification. Individual secondary nested PCRs (nPCR) were performed using
221 marker-specific primers with an overhang sequence in the 5' end and 25 cycles, enabling multiplexing of amplicons
222 per sample. nPCR products were purified, quantified, and normalised at 15 ng/µL using QIAGEN MinElute 96 UF PCR
223 Purification Kit (QIAGEN, Germany) and Quant-iT PicoGreen® dsDNA kit (Thermo Fisher Scientific, USA), respectively.

224 Normalised nPCR products were pooled and performed index PCR (iPCR) using long fusion primers with P5/P7
225 adapters, index and overhang sequences in the backbone, limited to 10 PCR cycles.

226 iPCR products were quantified and normalised at 20 ng/µL, then combined into pools of equal molarity. Long fusion
227 primers (<200 nt) and long non-specific PCR products (>400 nt) were removed from the final library by double size
228 exclusion using 0.55 and 0.25 volumes of NucleoMag® NGS beads, respectively (Macherey-Nagel, Germany). Each pool
229 was normalised to 10 nM and combined into a final sequencing library. Correct amplicon sizes in library pools were
230 confirmed by Agilent D5000 ScreenTape System (Agilent Technologies, USA). The final library was sequenced on an
231 Illumina MiSeq platform in paired-end mode using the MiSeq reagent kit v3 (600 cycles; 2 × 300 bp) with 15% spike-in
232 of Enterobacteria phage *PhiX* control v3 (Illumina) at the Walter and Eliza Hall Institute Genomics Core (Melbourne,
233 Australia).

234 **Analysis of assay sensitivity: Serial dilution of samples, natural and mock mixed infections**

235 The dynamic range and limit of detection (LOD) of PvAmpSeq markers were estimated by two approaches: i) serial
236 dilution of one clinical *P. vivax* sample at 802, 80.2, 40.1, 8.02, 4.01, and 0.8 parasites/µL, and ii) evaluating the
237 detection of minority clones in mock mixed infections. We considered a marker successfully sequenced when it had
238 >1000 reads per sample. We determined the last sample dilution detected by the assay as the last sample with at least
239 7 of 11 successfully sequenced markers (40% of missingness). Samples with fewer than 7 of 11 successfully sequenced
240 markers were filtered out due to low-quality amplification.

241 To determine the LOD of minority clones of the PvAmpSeq assay, we performed the assay on both natural and mock
242 mixed *P. vivax* infections. For this study, we define a "clone" as a unique microhaplotype detected within a sample.
243 The LOD was established as the lower within-host frequency or the highest dilution in which a minority clone was
244 detected, in natural or mock mixed *P. vivax* infections, respectively. As part of PvAmpSeq optimisation, we selected 6
245 markers (Chr03, Chr05, Chr06, Chr07, Chr08 and Chr13). To specifically measure the noise and detectability of minority
246 clones, we then performed the assay in duplicates using the 6 markers on *P. vivax* natural infections from Papua New
247 Guinea (n = 8) and Peru (n = 12). Two monoclonal *P. vivax* DNA isolates confirmed by WGS from the Solomon Islands
248 trial were mixed in different proportions: 1:1, 1:10, 1:50, 1:100, 1:500, 1:1000, 10:1, 50:1, 100:1, 500:1, 1000:1 and
249 sequenced at all 11 markers. We also evaluated the detection of minority clones by artificially creating mixed infections
250 from sequencing data using the Biostrings[41] and ShortRead[42] R packages. We generated artificial amplicon datasets
251 from a sub-selection of the raw FASTQ sequences generated in this study from 14 monoclonal *P. vivax* samples

252 sequenced at the 11 markers. We created artificial sequence data for each marker with known MOI and clone mixture
253 proportions by randomly selecting the sequence from two samples with 10 different mixture proportions (0.1%, 0.5%,
254 1%, 2%, 3%, 4%, 5%, 10%, 20%, and 50%) and 7 different read counts (100, 200, 500, 1000, 2000, 5000, and 10000).
255 For read counts of 100, 200, and 500, the mixture proportion started at 1% because we could only extract the integer
256 sequence from two samples. For each marker, we only artificially mixed two samples of distinct microhaplotypes and
257 non-missing reads. Additionally, to generate more realistic amplicon datasets, we also created artificial sequence data
258 that reflected random sampling error by utilising binomial sampling with 10 different probabilities (mixture
259 proportions as above) and 7 different read counts (as above) and repeated this 50 times. We then randomly selected
260 20 combinations of two distinct samples from each marker.

261 **Sequencing read analysis and haplotype calling**

262 Sequencing reads were analysed using the R package AmpSeqR version 0.1 (https://github.com/bahlolab/AmpSeqR).[33]
263 Sequencing reads were demultiplexed by sample and by amplicon. The overlapping sequences of paired reads were
264 merged, and samples with a read coverage of <1,000 reads per sample were excluded from the analysis. Index,
265 overhang sequences, and primer sequences were removed by trimming from the forward and reverse reads. In this
266 study, a microhaplotype was defined as an amplicon sequence variant at a given locus. The minor allele frequency
267 (MAF) was calculated for every single nucleotide in the given dataset, and then SNPs below 0.1% in frequency were
268 removed to exclude PCR and sequencing errors. In microhaplotypes resulting from insertion and deletion (indels), such
269 as homopolymer regions (>3 repeated bases, based on the reference sequence, e.g., "AAAA"), the sequence was
270 adjusted to have the reference number of repeats. Microhaplotypes with low sequence identity to the *P. vivax* P01
271 reference genome (<75%) or with a frequency < 1%, and chimeric and singleton reads were excluded from further
272 analysis. A marker was considered successfully sequenced if the number of reads in a given sample was over 1000
273 reads and passed the criteria described above. Microhaplotype calling required a minimum of 5 reads coverage per
274 locus, a within-host haplotype frequency of ≥ 1%, and an occurrence of this microhaplotype in ≥ 2 samples over the
275 entire dataset. All amplicon sequencing data are available under accession numbers SAMN43387238 to
276 SAMN43387533 at the Sequence Read Archive (SRA), and the associated BioProject ID is PRJNA1153071.
277 Microhaplotype sequences were also deposited in the open-access Github repository:
278 https://github.com/jrosados/PvAmpSeq.

279 **Population-level and within-host diversity estimates**

280 The expected heterozygosity (H_e) was calculated for each locus in the given dataset as described elsewhere.[43] The
281 within-host microhaplotype frequency was calculated as the number of reads per microhaplotype per locus over the
282 sum of all reads per locus in a sample. Multiplicity of infection (MOI) was calculated as the highest number of distinct
283 microhaplotypes per locus across all loci in a given sample.

284 **Reproducibility of PvAmpSeq data and comparison with available microsatellite data**

285 As part of the optimisation of PvAmpSeq, we leveraged the availability of two sample types from the Solomon Islands
286 ACT-Radical clinical trial: red blood cell pellets and dried blood spots from the same individual, collected at the baseline
287 visit. We compared the microhaplotype marker coverage and MOI estimates for 17 patients with both types of
288 samples.

289 In addition, five DNA samples from the Peruvian cohort had matched microsatellite genotyping data based on 16
290 markers published by Manrique *et al*.[44] We also compared the PvAmpSeq MOI data with MOI estimates based on
291 microsatellite data.

292 **Classification of infections into low, medium and high IBD**

293 We used the *dcifer* R package to calculate identity-by-descent (IBD) IBD r^ and the IBD $r\hat{}_{total}$ (i.e., inferred shared
294 ancestry) between polyclonal infections using a statistical framework for inference that accounts for the complexity
295 of infection (COI) and population-level allele frequencies (in our case, microhaplotype frequencies).[45] Briefly, we first
296 estimated naive COI, and then population-level haplotype frequencies were adjusted for the estimated COI based on
297 our data. *Dcifer* provides estimates of r^, the relatedness between two samples, and performs a likelihood-ratio test
298 to test the null hypothesis that two samples are unrelated (H0: r^ or IBD = 0) at a significance level of $\alpha = 0.05$, adjusted
299 for a one-sided test. For all pairs of related samples where we reject the null hypothesis, this provides statistical
300 confidence that two pairs of samples are significantly related. In addition, in the case of samples with COI>1 we also
301 estimate both *M'*, which is the number of related *clone* pairs between both samples, and $r\hat{}_{total}$, which represents the
302 'total' or overall relatedness between all clones. The method makes the simplifying assumption that there is no within-
303 host relatedness between clones in an infection. Based on IBD estimates, infections were considered as low (IBD
304 <0.25), medium (IBD: 0.25–0.5), and high IBD (IBD ≥0.5). We used the *ggraph* R package to generate network plots
305 and visualize the relatedness between samples.

306 **Classification of recurrences into relapse, recrudescence, and reinfections**

307 We used the recently developed *Pv3Rs* R package, which uses a probabilistic model-based framework to compute the
308 posterior probabilities that recurrent *P. vivax* infections are recrudescences, relapses, or reinfections based on genetic

309 data.[46] The model accounts for IBD of parasite clones within and between episodes within a Bayesian framework that
310 requires as input population-level allele frequencies (in our case, microhaplotype frequencies) and prior probabilities
311 for each recurrence classification state. The model computes the probabilities of sequences of recurrent states over
312 recurrent episodes conditional on the genetic data on a per-participant basis and outputs the per-recurrence
313 probabilities of each state (recrudescence, relapse, and reinfection). We report individual-level posterior probabilities
314 for each recurrence state alongside aggregated summaries of the mean posterior probability and standard deviation
315 across all recurrences for each state, thereby propagating uncertainty into population-level estimates. As per the
316 recommendations for the current implementation of the model, we only ran the model on participant samples where
317 the total COI across episodes was ≤ 8. This removed only one participant from Solomon Islands (AR-359, total COI=11)
318 and none from Peru.

319 To inform our prior probabilities for recurrence states of recrudescence, relapse, or reinfection in the Solomon Islands
320 clinical trial samples, we consider different prior probability distributions on a per-patient, per-episode basis based on
321 whether they received PQ or not, and days since the baseline episode and receiving treatment. Given there is no
322 reported evidence suggesting widespread resistance to ACTs in the Solomon Islands, assume the probability of
323 recrudescence is low but not negligible and constant over time and treatment groups We specified time-dependent
324 priors reflecting expected changes in the relative contribution of relapse and reinfection during follow-up, since
325 Solomon Islands is still a moderate transmission setting. In addition, fast-relapsing strains like the Chesson phenotype
326 reported in the Western Pacific, relapses can occur within <2 months, sometimes even <30 days, with multiple relapses
327 (>3) possible. [47,49] Accordingly, we considered three windows of time since treatment: ≤30 days, >30 days and < 90
328 days, ≥90 days and specified slightly higher relapse probability in early follow-up (<30 days), with a gradual shift toward
329 a higher probability of reinfection with increasing time since treatment. With respect to the treatment administered
330 in each arm, the original ACT-Radical clinical trial randomized participants into three treatment arms (AL; AL-PQ;
331 dihydroartemisinin-piperaquine+PQ [DP+PQ]),[31] however we considered only whether the participant received PQ or
332 not due to small sample sizes. The trial results demonstrated that both PQ arms had significantly reduced rates of
333 recurrences compared to the AL control arm, however PQ clinical efficacy was relatively low in both the AL+PQ and
334 DP+PQ arms (~34-44%) so we assumed that relapses were still likely despite PQ administration.[31] In PQ-treated
335 participants, we specified slightly lower relapse probabilities than in AL-treated participants to reflect partial

336 hypnozoite clearance, while still allowing for substantial relapse given the observed modest PQ efficacy in the original
337 trial. See Supplementary Table S7 for details on the prior probabilities we used.

338 For the Peru cohort, which was an observational community study where participants resided in two communities
339 (Cahuide and Lupuna), participants did not receive 'baseline' treatment or treatment throughout the study, meaning
340 that untreated persistent infections were possible. However, Pv3Rs is not designed to model persistent infections and
341 assumes recurrence states are mutually exclusive (either relapse, recrudescence or reinfection). When fit to the data
342 from Peru, Pv3Rs is misspecified and the state of recrudescence is ill-defined. In addition, recurrence states are liable
343 to overlap (e.g., an infectious mosquito bites a person with an untreated relapse, leading to persistent relapse plus
344 reinfection). To work around this misspecification, we can reinterpret Pv3Rs's recurrence state definitions as follows:
345 Pv3Rs recrudescence = persistence without added relapse or reinfection; Pv3Rs reinfection = reinfection without
346 persistence; Pv3Rs relapse = everything else, e.g. (relapse without persistence) OR (persistence AND reinfection) etc.
347 Prior work from the same community cohort has shown during 12-months of follow-up (which is similar to our study
348 period), relapses accounted for a slightly higher proportion of PCR-positive recurrences in Cahuide compared to
349 Lupuna (48% vs 35%), however these modelled outputs were not based on genetic data.[34] We therefore assumed most
350 recurrences in this setting are likely due to relapse or reinfection rather than recrudescence, with a slightly higher
351 probability of relapses in participants living in Cahuide (0.45) compared to Lupuna (0.33) (Supplementary Table S8).

352 To estimate population-level microhaplotype frequencies, we used only the subset of baseline samples for the
353 Solomon Islands clinical trial samples, but all samples for the Peru cohort. In the case of the Solomon Islands, we opted
354 for this approach to minimise the potential bias from within-host selection of recrudescent parasites, which might
355 distort microhaplotype frequency estimates if post-treatment samples were included. In the Peru cohort, we used all
356 samples to provide a broader representation of the circulating parasite population because most recurrences are
357 presumed to be reinfections or relapses (both drawn from the broader mosquito population).

358 We performed a series of sensitivity analyses to better understand the limitations of Pv3Rs and the potential impact
359 on our results. We explored the impact of inclusion/exclusion of samples for estimation of population-level
360 microhaplotype frequencies in the case of the Solomon Islands cohort and used all samples (baseline and follow-up)
361 to estimate population-level microhaplotype frequencies, which did not impact the classification of samples. We also
362 explored the impact of uniform and non-uniform priors on recurrence classification state. We did this in two ways: by
363 skewing the prior probability completely to one classification state (e.g. prior probability of reinfection = 0.95; prior

364 probability of recrudescence = 0.025; prior probability of relapse = 0.025, for all combinations) as well as a uniform
365 prior assuming equal probabilities (prior probabilities of reinfection = 0.33; recrudescence = 0.33; relapse = 0.33)
366 (Supplementary table S9).

367 To estimate the false discovery rate (FDR) of relapses and recrudescences (i.e., non-reinfections), we performed a
368 simple perturbation of infection pairs. We randomised infection pairs (i.e., selecting entire 'infection sets' of
369 microhaplotypes and randomly pairing them to another infection set), ensuring that pairs were not derived from the
370 same participant and imposing a time order such that the recurrent infection always occurred after the first infection.
371 In the Solomon Islands dataset, we randomised baseline samples with follow-up samples, and in the Peru dataset, we
372 randomised all samples. This generated a 'null' data set of inter-participant infection pairs where paired infections
373 should neither represent relapses nor recrudescences. We then ran Pv3Rs on the null data set using the default
374 uniform prior (because we had low sample sizes to appropriately randomize within specific groups, e.g. treatment
375 arm, time windows between episodes, community) and computed the FDR as the mean posterior probability estimate
376 of non-reinfections (1 – the probability of reinfection averaged over inter-participant pairs). We ran 100 replicates and
377 calculated the mean FDR and 95% confidence interval across replicates for each cohort.

378 The expected FDR is not zero because Pv3Rs is designed to return a non-zero posterior probability of both reinfection
379 and relapse when genetic data are consistent with recurrent parasites that are genetically unrelated to those detected
380 previously. For each replicate, we computed the minimum FDR as one minus the upper bound on the posterior
381 probability of reinfection averaged across inter-participant pairs. Different data sets have different minimum FDRs
382 because different MOI vectors induce different posterior bounds; a look-up table of posterior bounds was computed
383 previously.[46] We then compare the mean FDR computed using posterior probabilities with the mean minimum FDR.

384 To assess how particular microhaplotypes might influence our posterior probability estimates of each recurrence state,
385 e.g., due to heterozygosity or number of alleles in the population, we iteratively re-ran the Pv3Rs analysis using
386 informative priors as described above but omitting one marker each time.

387 Quantification and Statistical Analysis

388 **Statistical analysis and data accessibility**

389 Categorical variables were compared using the two-sided Fisher's exact test or χ2 test when required. Continuous
390 covariates were compared using two-sided Mann-Whitney, Kruskal-Wallis, or T-test when required. Relationships
391 between parasite density and read counts were tested using the Pearson correlation coefficient, and *p-values* were

392 adjusted by the Benjamini-Hochberg method. The success rate per marker was defined as the number of sequenced
393 samples that met the marker criteria divided by the total number of samples with a valid number of reads (>1000
394 reads per sample). We used the d_0 distance metric, as reported by Mideo et al.,[48] to quantify the replicability of
395 microhaplotype frequency estimates between technical replicates. The association between clonality (monoclonal and
396 polyclonal) and the days since preceding infection was evaluated using a two-sided Mann-Whitney test. To evaluate
397 the association between the change of MOI across different events from the same individuals (increase, decrease or
398 no change) and the median time since preceding infection, we used a Kruskal-Wallis test. All statistical analyses were
399 performed using R 4.1.0 (https://www.r-project.org/). Original data, R scripts, and algorithms developed in this study
400 are accessible in the repository https://github.com/jrosados/PvAmpSeq. The sample and patient IDs of the original
401 databases were not known to anyone outside the research group. De-identified datasets were generated during the
402 current study and used to make all figures available as supplementary files or tables.

403

404 # Results

405 **PvAmpSeq microhaplotype marker selection**

406 Of the 354 samples processed from PvGV, 200 high-quality WGS sequences from 6 countries (Cambodia, Colombia,
407 Mexico, Papua New Guinea, Peru, and Thailand) were searched for all regions that contained at least 4 SNPs within a
408 window of 140 bp. All successful polymorphic regions were then ranked by expected heterozygosity within each
409 country, with the highest mean-ranked microhaplotype being selected for each of the 14 chromosomes (Figure S1–
410 S2). Although we excluded the majority of the hypervariable sub-telomeric regions of PvP01 genome sequence,
411 microhaplotypes from Chr06 and Chr12 were selected but then excluded during the PCR optimisation as they were
412 located in the proximity of hypervariable sub-telomeric pir genes. Chr04 was excluded due to the low amplification
413 success in Solomon Islands samples. Our panel included 11 microhaplotype markers or loci across 11 chromosomes.

414 The final panel of PvAmpSeq microhaplotype markers comprised three loci encoding highly polymorphic surface
415 antigens such as Merozoite Surface Protein 1 (MSP1, Chr07, PVP01_0728900), Merozoite Surface Protein 3 (MSP3.3,
416 Chr10, PVP01_1031500) and Apical Membrane Antigen 1 (AMA1, Chr09, PVP01_0934200); proteins involved in
417 reticulocyte invasion, Reticulocyte Binding Protein 2a (RBP2a, Chr14, PVP01_1402400); enzymes such as Protein
418 Tyrosine Phosphatase putative (PTP2, Chr01, PVP01_0113700), Glyoxalase I-Like Protein (GILP) putative (Chr11,
419 PVP01_1144200); pseudogenes like Lysophospholipase putative (Chr02, PVP01_0201300); and putative proteins of
420 unknown function such as STP1 protein (Chr05, PVP01_0533300), conserved Plasmodium protein (Chr03,

421 PVP01_0302600 and Chr13, PVP01_1346800) and Plasmodium exported protein (Chr08, PVP01_0838000). These
422 genes contain both SNPs and indels (Text S1).

423 **Application to samples from two cohort studies**

424 A total of 492 (Solomon Islands, n = 218; Peru, n = 274) samples were sequenced for the validation of the PvAmpSeq
425 assay. 196 samples were filtered out due to a low number of reads (<1,000 reads per sample) or low identity sequences
426 (Solomon Islands, n = 71; Peru, n = 125). Discarded samples and successful samples had a median parasite density of
427 14.4 parasites/µL of DNA [IQR: 5.63–39.5] and 232 parasites/µL [IQR:34.2–1240], respectively. Additionally, samples
428 with more than 40% (5 out of 11 loci) of missingness were discarded (Peru, n = 9), as were 10 samples from the
429 Solomon Islands trial, due to sequencing failure of their baseline infection. Negative DNA samples and negative
430 template controls included in sequencing runs yielded <100 reads and were filtered out.

431 The remaining 275 samples selected for downstream analysis corresponded to 77 participants from the Solomon
432 Islands and 93 participants from Peru. Of the Solomon Islands participants, 41 had available samples from 1 up to 6
433 PCR-detected recurrent infections (total 58 samples), whereas only 40 Peruvian participants had follow-up samples,
434 corresponding to 1 or 3 recurrent infections (total 47 samples). The median age of the participants was 10.1 years
435 [IQR: 7.42–14.4] and 36.7 [18.0–51.5] for the Solomon Islands and Peru, respectively (Table 1). There was no significant
436 difference between the parasite density of baseline and follow-up infections for both cohorts ($p > 0.05$). As expected
437 for the clinical trial, febrile infections were more frequent at baseline for the Solomon Islands cohort ($p < 0.05$).

438 **Data processing and read coverage**

439 Reads were demultiplexed and filtered using AmpSeqR.[33] After discarding PCR artefacts, the rate of success per locus
440 went from 0.70 to 1 (Table S2). The median success rate amongst follow-up samples was slightly lower than for
441 baseline samples but still around 0.90 for both cohorts (Solomon Islands; baseline median: 0.99[IQR: 0.97–1.00], vs
442 follow-up median: 0.91[0.91– 0.95], $p < 0.05$; Peru; baseline median: 0.98 [0.80-0.98], vs follow-up median: 0.89 [0.82–
443 0.93], $p > 0.05$). The median read coverage per marker was 4309 [2051-8129] and 4752 [2535.5–7524] for the Solomon
444 Islands and the Peruvian cohort, respectively. Chr07 had the highest median read coverage per sample in both cohorts
445 (9774, [4672.2–9964] for the Solomon Islands and 8734 [5560.5–9857.2] for Peru), whereas Chr01 had the lowest
446 median coverage read (1763 [960–2326] in the Solomon Islands; and 2376 [1606–4180] in Peru) (Figure 1A).

447 No significant correlation was found between the sample parasite density (parasites/µL) and the number of reads per
448 marker (Pearson's *r* range = -0.23–0.16, adjusted p range = 0.17–0.94) (Figure 1B). Samples with <10 parasites/µL were
449 amplified with variable read coverage per marker (median: 4590 [2574–8499]). The high variance seen in each parasite

density group suggested that the DNA quality affected the amplification performance. On the other hand, detection of a control sample (AR-246) was possible only when parasite density was >40 parasites/µL. Microhaplotypes were detected at dilutions of 40.1, 80.2, and 802 parasites/µL for the control sample (Figure 1C). Control sample dilutions with ≤8.02 parasites/µl were poorly sequenced for most of the loci (<60 reads). Chr13 did not successfully amplify in the control sample and was excluded from this analysis. We detected one microhaplotype per locus in the AR-246 control sample for all dilutions, except at the highest dilution of 802 parasites/µL, where two microhaplotypes were detected in marker Chr09, one of which had a very low microhaplotype frequency (0.018) (Figure S3). This microhaplotype could be a true microhaplotype since it was also detected in other samples in this dataset and with high frequency. This indicates that, as expected, higher parasite densities can more accurately determine the complexity and diversity of sample infections.

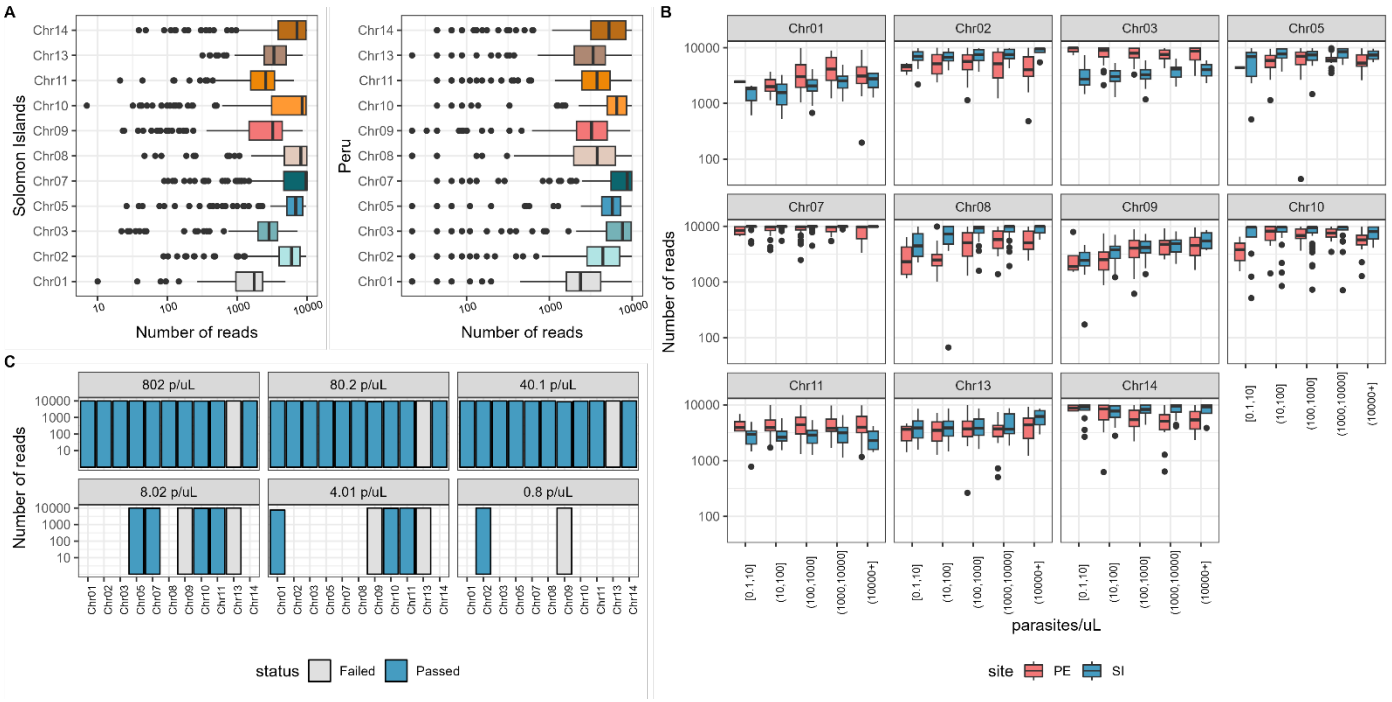

Figure 1. Marker coverage and sample parasite density. (A) Number of reads per marker on field samples. (B) Number of reads and parasite density of field samples. (C) Limit of detection for parasite density; in blue: markers that passed the quality control step; in grey: markers that failed the quality control step; empty bars: markers with no successful PCR amplification.

Limit of detection for minority clones

The PvAmpSeq demonstrated high replicability and sensitivity for detecting minority *P. vivax* clones. We performed experimental replicates using 6 markers (Chr03, Chr05, Chr06, Chr07, Chr08 and Chr13) in natural infections from Papua New Guinea (n = 8) and Peru (n = 12), to measure the noise and detectability of minority clones. We found that minority clones with a within-host frequency of >1% were consistently detected in both technical duplicates providing confidence in a low LOD (Figure S4). Replicability was quantified using the d_0 distance metric (Mideo et al.). While minority microhaplotypes were detected across duplicates in polyclonal samples, their estimated relative within-host

471 frequency varied between markers, and some minority clones were not detected by certain markers despite aiming
472 for 5000 reads per marker, highlighting marker-specific performance differences in quantifying allele frequencies.

473 Two monoclonal samples (AR079 and AR093) from the Solomon Islands trial were selected to mimic a mixed infection.
474 DNA samples were normalised at 100 parasites/µL and combined in the following ratios: 1:1, 1:10, 1:50, 1:100, 1:500,
475 1:1000, 10:1, 50:1, 100:1, 500:1, and 1000:1. The results of the mock mixed infections are shown in Figure 2A. Analyses
476 were restricted to informative PvAmpSeq markers with distinct microhaplotypes between samples: Chr01, Chr02,
477 Chr03, Chr05, Chr09, and Chr14. Markers Chr07, Chr08, Chr10, and Chr11 were not included because both samples
478 had the same microhaplotype in these loci. The correct minor microhaplotype was detected in most mixtures only at
479 1:1 (50%), 1:10 (10%), and 10:1 (10%) mixture proportions for Chr01, Chr02, Chr09, and Chr14; however, the
480 proportion detected often did not match the defined mixture ratio. Minority clones at 1:50 (2%) were detected for
481 Chr02, indicating a low LOD for this particular marker. In most samples, only microhaplotypes from the major clone
482 were detected. We examined the minor clone sequences in the raw sequence data for each sample and found that
483 the minor clone sequence coverage was extremely low (less than 5 reads compared to over 20,000 reads in total),
484 which resulted in the inability to detect the minor clones. These results suggest a biased PCR amplification of certain
485 clones and a marker-specific variability in quantification. In some samples, we detected singleton microhaplotypes
486 with very low frequencies that were not AR-079 or AR-093 microhaplotypes, which likely represent false positives
487 (Figure S5). We compared the sequences of these major and minor microhaplotypes and found that these minor and
488 major microhaplotypes differed in only one position. These microhaplotypes are likely to be systematic sequencing
489 errors, with the base-call errors generally occurring at the same genomic position from different sequence reads.46
490 Systematic errors are often mistaken for heterozygous sites in individuals or SNPs in population analysis.

491 We also examined the LOD of artificially mixed infections by determining the minority clone detectability success in
492 silico. At the highest read counts (5,000 and 10,000), the minor clone was robustly detected at a clone relative
493 frequency as low as 0.5% up to 50% for all amplicon markers; however, when read counts were <1,000, the minor
494 clone was only detected accurately when the relative frequency was >10% (Figure 2B). Regardless of the data being
495 generated with the same mixture ratios and read counts, there were substantial differences in the detectability of the
496 minor clone based on the microhaplotype marker. For example, at a read count of 10,000 and a minor clone relative
497 frequency of 0.1%, three markers had 100% success in detecting the minor clone (Chr03, Chr07, and Chr10). In
498 contrast, there were very low success rates for markers Chr01, Chr08, Chr11, Chr13, and Chr14, ranging from 0% to

29%. We also created the artificially mixed infections following a binomial distribution to reflect a more realistic random sampling error and found similar results to those above (Figure S6). Combining both in vitro and in silico results of mixed infections, we thus set 2% as the lower LOD for minority clones of PvAmpSeq and recommend at least 10,000 reads per microhaplotype amplicon for robust minor clone detection (assuming frequency may be as low as 2%). If the minor clone relative frequency is expected to be around 10%, we recommend at least 1,000 reads.

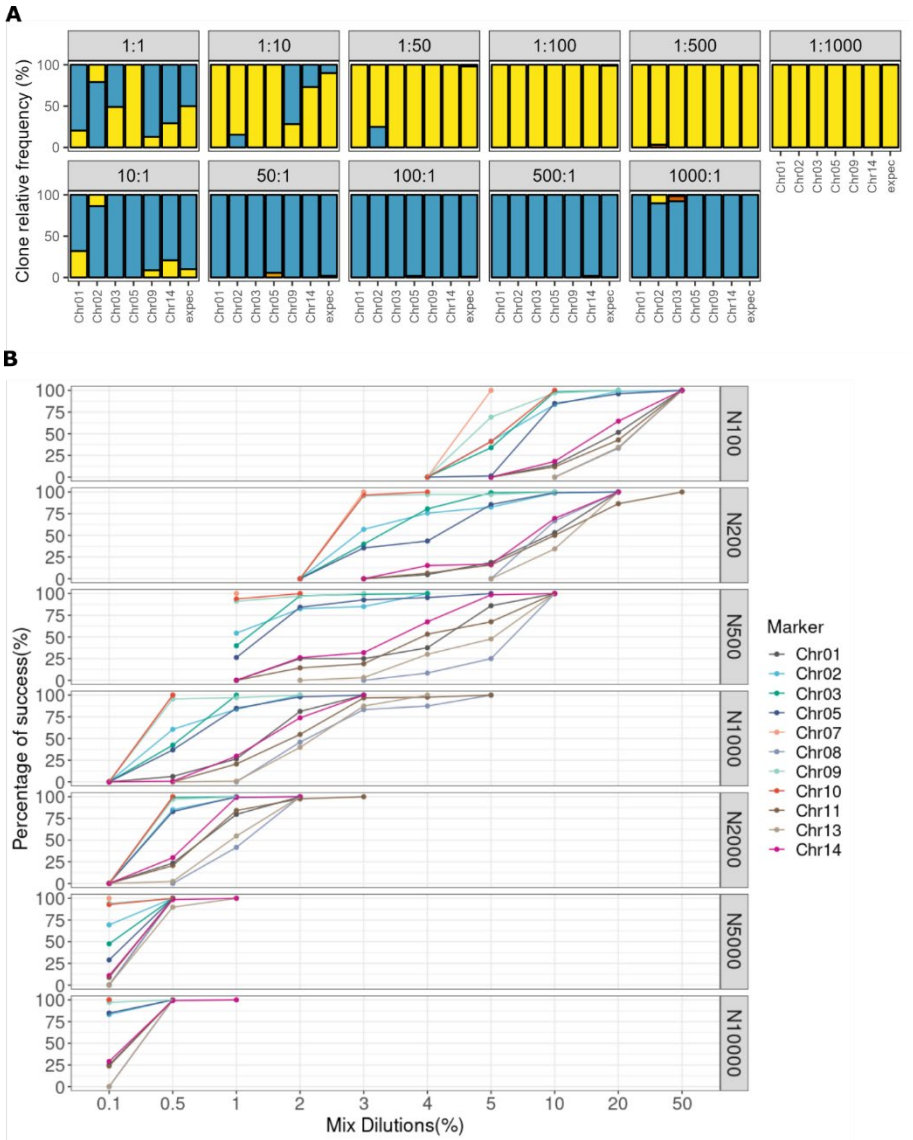

Figure 2. Detection of minority clones in mock and artificial mixed infections. (A) The Y-axis shows the sample ratios detected in mock mixed infections. The X-axis shows the markers grouped by expected sample ratios in mock infections (1:1, 1:10, 1:50, 1:100, 1:500, 1:1000, 10:1, 50:1, 100:1, 500:1 and 1000:1). In blue: clones from sample AR079; in yellow: clones from sample AR093; in red or orange: contaminant clones. expec: expected results from mock mixed infections. Markers sharing the same microhaplotypes between samples are not displayed. (B) The detectability of the minor clone under different numbers of reads and artificial mixture ratios. The X-axis represents the mixture dilutions (%), and the Y-axis represents the success rate (%) of detecting the minor clone. Coloured by amplicon marker.

Exploring population and within-host genetic diversity metrics using PvAmpSeq

The microhaplotype markers had high diversity in both sample sets, with the mean expected heterozygosity (H_e) of the 11 markers 0.70 for the Solomon Islands samples and 0.65 for the Peruvian samples. We found approximately half of the markers had high He ≥ 0.70 (7/11 markers in the Solomon Islands; 5/11 markers in Peru), but the markers with the highest heterozygosity differed in each cohort except for Chr05 and Chr07, which had high He in both (Figure 3A)

but different microhaplotype frequencies (Figure 3B). The remaining markers had low- to moderate heterozygosity, ranging from 0.29 to 0.69 (Figure 3A). High diversity markers (He ≥ 0.70) had a median of 7 alleles (range: 4–43) and 13 microhaplotypes (range: 5–13) in the Solomon Islands and a median of 6 alleles (range: 3–34) and 7 microhaplotypes (range:5–7) in Peru (Table S3).

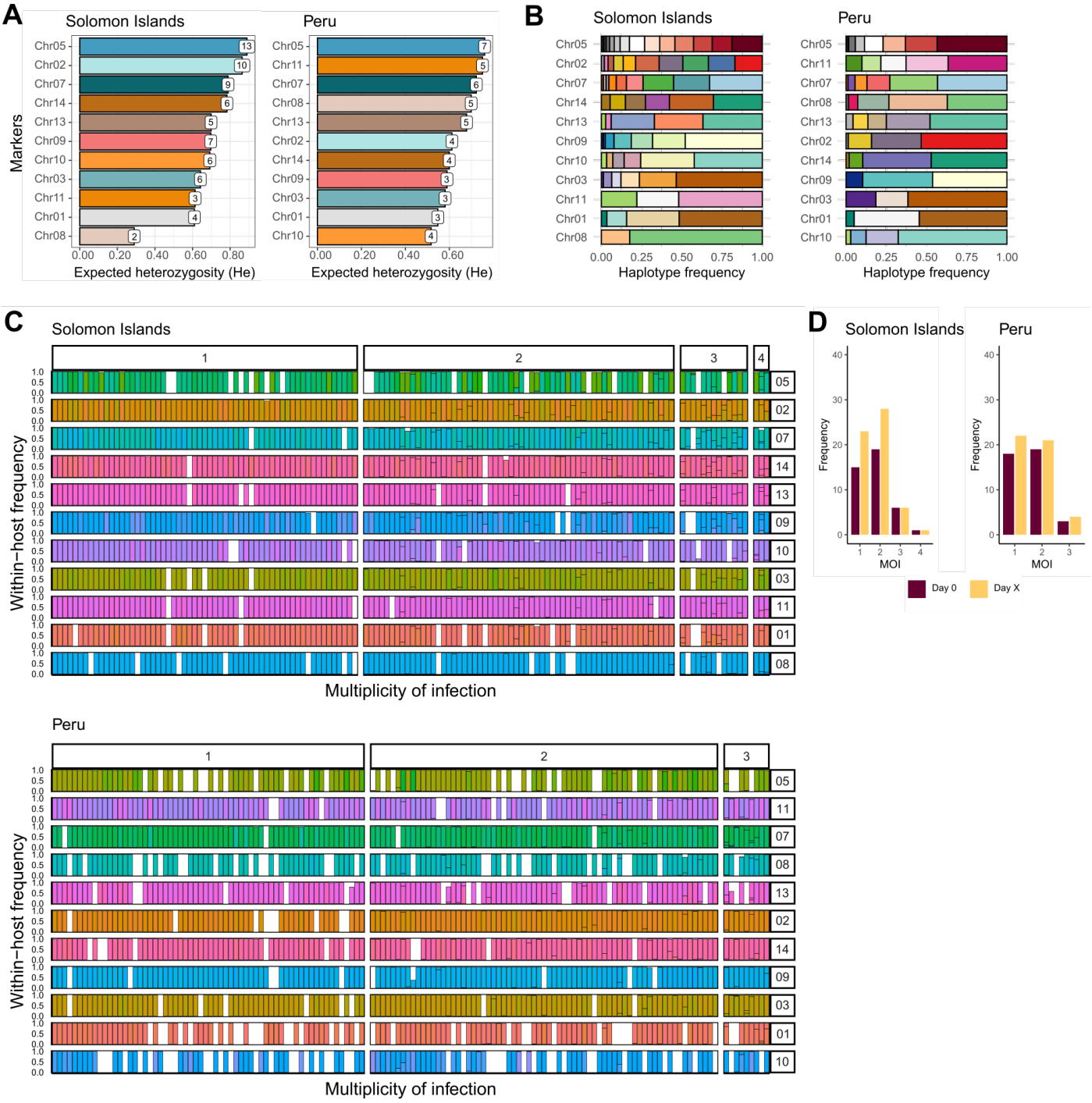

Figure 3. Genetic diversity of markers and multiplicity of infection (MOI) of validation samples. (A) Markers were sorted by descending H_e. He: Expected heterozygosity calculated as the number of microhaplotypes per marker divided by microhaplotype frequency on Solomon Islands (n = 135) and Peruvian samples (n = 140). The number of microhaplotypes per marker is indicated on top of each bar. (B) Microhaplotype frequency per marker estimated for the Solomon Islands and Peruvian samples. Each colour indicates a different microhaplotype. (C) The estimated MOI in field samples as the highest number of distinct microhaplotypes by all markers. The Y-axis shows the within-host frequency of microhaplotypes per sample, calculated as the percentage of microhaplotype reads per sample. The X-axis shows the samples sorted by estimated MOI. Every sample is represented by a vertical bar. (D) Distribution of MOI in paired samples, where Day 0 represents the baseline infection (Solomon Islands, n = 41; Peru, n = 40) and Day X the day of recurrent infection (Solomon Islands, n = 58; Peru, n = 47).

529 Using the highest number of distinct microhaplotypes detected by all markers, we estimated the MOI in both cohorts.
530 Out of 135 samples in the Solomon Islands cohort, 59 had a maximum MOI = 1, 60 samples had a maximum MOI = 2,
531 13 samples had MOI = 3, and 3 samples had MOI = 4 (Figure 3C). In the Peruvian cohort, out of 140 samples, 62 had a
532 maximum MOI = 1, 69 samples had a maximum MOI = 2, and 9 samples had MOI = 3 (Figure 3C). No association was
533 found between the maximum MOI obtained in baseline samples and participant's age (Kruskal-Wallis test, Solomon
534 Islands $p = 0.986$, Peru $p = 0.672$; Figure S7), nor with the presence of fever ($\chi 2$ test, Solomon Islands $p = 0.744$, Peru
535 $p = 0.823$; Figure S8). There was no significant difference in MOI at baseline compared to follow-up in either cohort
536 (Solomon Islands, baseline mean MOI = 1.83 vs follow-up mean MOI = 1.74, two-sided Mann-Whitney test, $p = 0.5997$;
537 Peru, baseline mean MOI = 1.62 vs follow-up mean MOI = 1.62, two-sided Mann-Whitney test, $p = 0.9244$) (Figure 3D,
538 Table S4). To test whether participants with polyclonal infections at baseline had faster times to first recurrence than
539 those with monoclonal infections at baseline, we compared the time to first recurrent infection of paired samples
540 stratified by MOI at baseline (MOI = 1 vs MOI ≥ 2). In both cohorts, polyclonal baseline infections (MOI ≥ 2) had
541 comparable times to first recurrent infection to monoclonal baseline infections (MOI = 1) (two-sided Mann-Whitney
542 test, Solomon Islands $p = 0.7555$, Peru $p = 0.0635$; Figure S9A). Likewise, the time to the next recurrent infection was
543 not affected by the change of MOI between recurrent infections (Kruskal-Wallis test, Solomon Islands $p = 0.3979$, Peru
544 $p = 0.4724$; Figure S9B).

545 As part of the assay validation, we used available microsatellite data for 5 Peruvian samples to compare MOI estimates
546 using microsatellite genotyping and PvAmpSeq. Three out of the five samples appeared to be polyclonal by PvAmpSeq,
547 whereas only one sample was previously reported as polyclonal by microsatellites (Table S5).

548 **Classifying recurrent infections using identity-by-descent and probabilistic estimates**

549 Paired samples were further analysed to identify whether recurrent infections exhibited high or low relatedness
550 relative to the baseline infection in the Solomon Islands trial or the first infection during the Peruvian community
551 cohort study period. Based on IBD estimates, in the Solomon Islands ACT-Radical clinical trial, 55.2% (32/58) of
552 recurrent infections had high IBD (IBD ≥0.5), while 41.4% (24/58) had low IBD (IBD <0.25) and 3.4% (2/58) had medium
553 IBD (IBD 0.25–0.5) (Figure 4A). A smaller proportion of recurrences had high IBD compared to baseline among people
554 who received primaquine at baseline, compared with people who did not, but without significant differences (68.2%
555 [15/22] vs 47.2% [17/36]; two-sided Fisher's exact test, $p = 0.3202$, Table S6).

556 In the Peruvian community cohort, 23.4% (11/47) of recurrent infections had high IBD, while 68.1% (32/47) had low
557 IBD and 8.5% (4/47) had medium IBD (Figure 4B). To evaluate whether recurrent polyclonal infections contribute to
558 increased IBD, we compared the frequency of polyclonal infections in both cohorts per IBD group. We did not find an
559 association between MOI and IBD of recurrent infections in either cohort (two-sided Fisher's exact test, Solomon
560 Islands $p = 0.1279$, Peru $p = 0.3754$; Table S6). Detailed microhaplotype data and IBD classification of recurrent samples
561 can be seen in Figure S10, S11, Text S2 and Text S3.

562 We found that IBD in recurrent infections changed with time for most of the recurrent episodes in both cohorts, with
563 a maximum number of five and three recurrences experienced by the same participant in the Solomon Islands and
564 Peru, respectively. For example, we found evidence that the participants in the Solomon Islands clinical trial who had
565 four and five recurrences had recurrences with low and high IBD, respectively, compared to the baseline infection,
566 (Figure 4C) and in Peru, most participants experienced recurrences with low IBD (Figure 4D). There was no clear
567 pattern with time to recurrence in the Solomon Islands clinical trial (Kruskal-Wallis test, $p = 0.218$; Figure 4E, see Figure
568 S12A for samples that failed sequencing). In Peru, infections with high IBD tended to happen within 100 days since
569 first infection (median 57 days [34-63]), compared to infections with low IBD that happened around a median of 188
570 days (range: 121-242)(Kruskal-Wallis test, $p = 0.017$; Figure 4F, see Figure S12B for samples that failed sequencing).

571 We evaluated the genetic relatedness (IBD estimates) of parasite isolates within and between transmission seasons
572 in both cohorts. Higher levels of relatedness were found in the Peruvian cohort in contrast to the Solomon Islands trial
573 (Figure S13), with possible clonal expansion (IBD ≥0.9) in the former. We detected more genetic clusters when
574 including all samples MOI ≥1 (IBD ≥0.9), which included isolates from different transmission periods within a year and

575 from different years.

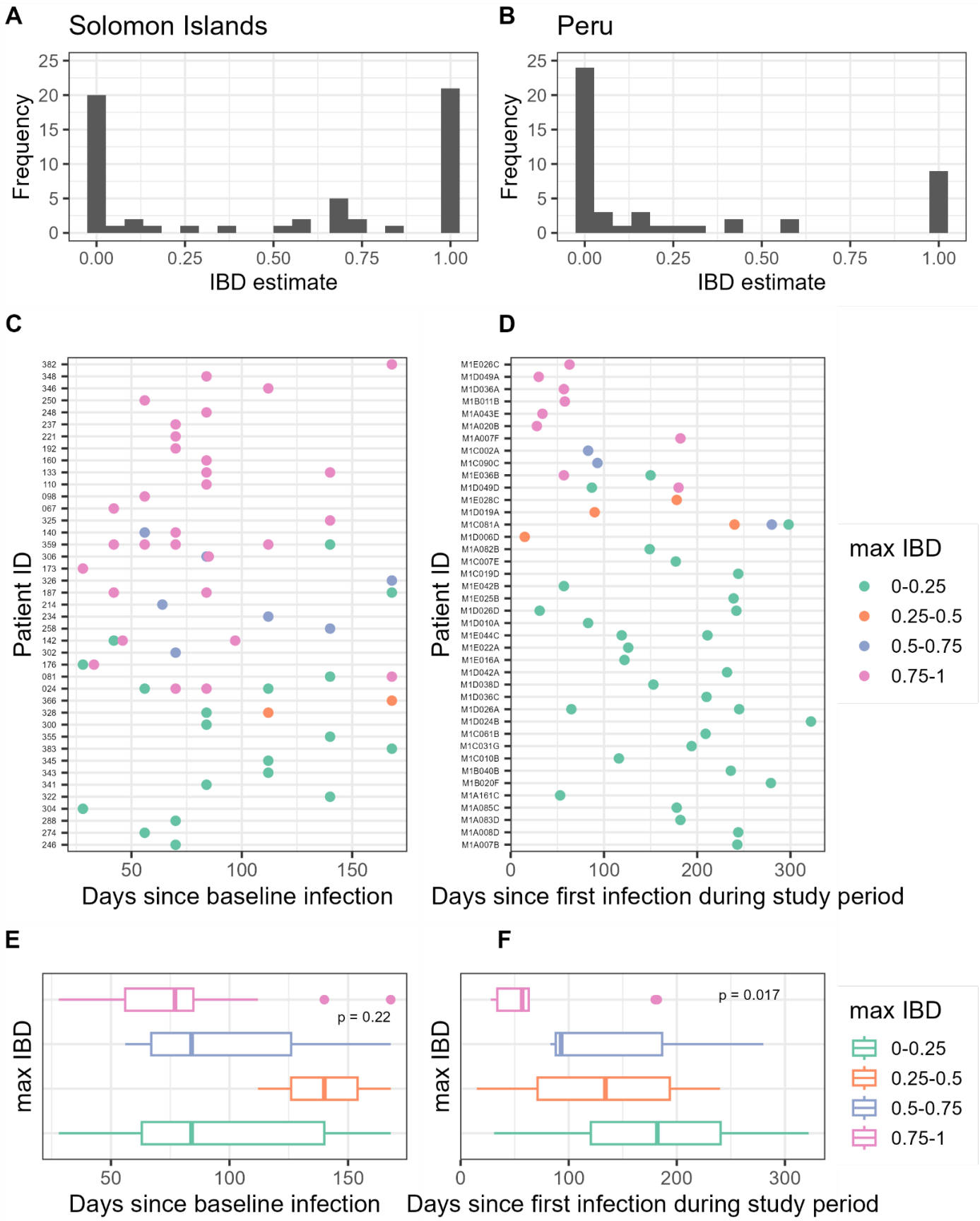

576

577 **Figure 4.** Classification of *P. vivax* recurrent infections with PvAmpSeq using IBD. (A-B). Distribution of IBD estimates in paired samples from the
578 Solomon Islands and Peru, comparing baseline and first recurrence pairs. (C-D). Maximum IBD between recurrence and preceding infection pairs
579 in the Solomon Islands and Peru. The X-axis shows the days since baseline (becoming infected), the Y-axis depicts each patient's infection over
580 time, and the colour represents the IBD estimate range for the infection pairs. (E-F). Association of time since baseline infection and maximum
581 IBD estimate in recurrence and preceding infection pairs. Baseline (Day 0) infections are not displayed for easier interpretation of plots.

582 We also performed probabilistic classification of recurrences using the Pv3Rs R package to provide further granularity
583 on probable recurrence states. For the Solomon Islands, we explored the most probable state of each recurrent
584 infection and found that, after accounting for uncertainty, 37.6% of participants experienced a probable reinfection
585 (standard deviation, SD 0.41), 16.4% experienced a probable recrudescence (SD 0.30) and 46.0% experienced a
586 potential relapse (SD 0.36) (Figure 5A, 5C). Among participants who experienced more than one recurrence, there
587 were different sequences of most probable states, e.g. AR-024 has most probable reinfection at first recurrence
588 followed by relapseand then a reinfection (Figure 5A). Interestingly, for this participant, the IBD estimates for
589 recurrences were all <0.25 compared to baseline but the maximum IBD of recurrences compared to all preceding
590 episodes were 0, 1, 1, and 0 supporting the probabilistic estimates of both reinfection and relapse (Figure 4C). A
591 sensitivity analysis using inter-participant episode pairs generated a mean FDR of 20.6% (95% CI: 20.1–21.1%) for the
592 Pv3Rs model. It exceeds a mean minimum FDR of 15.7% by 4.9.

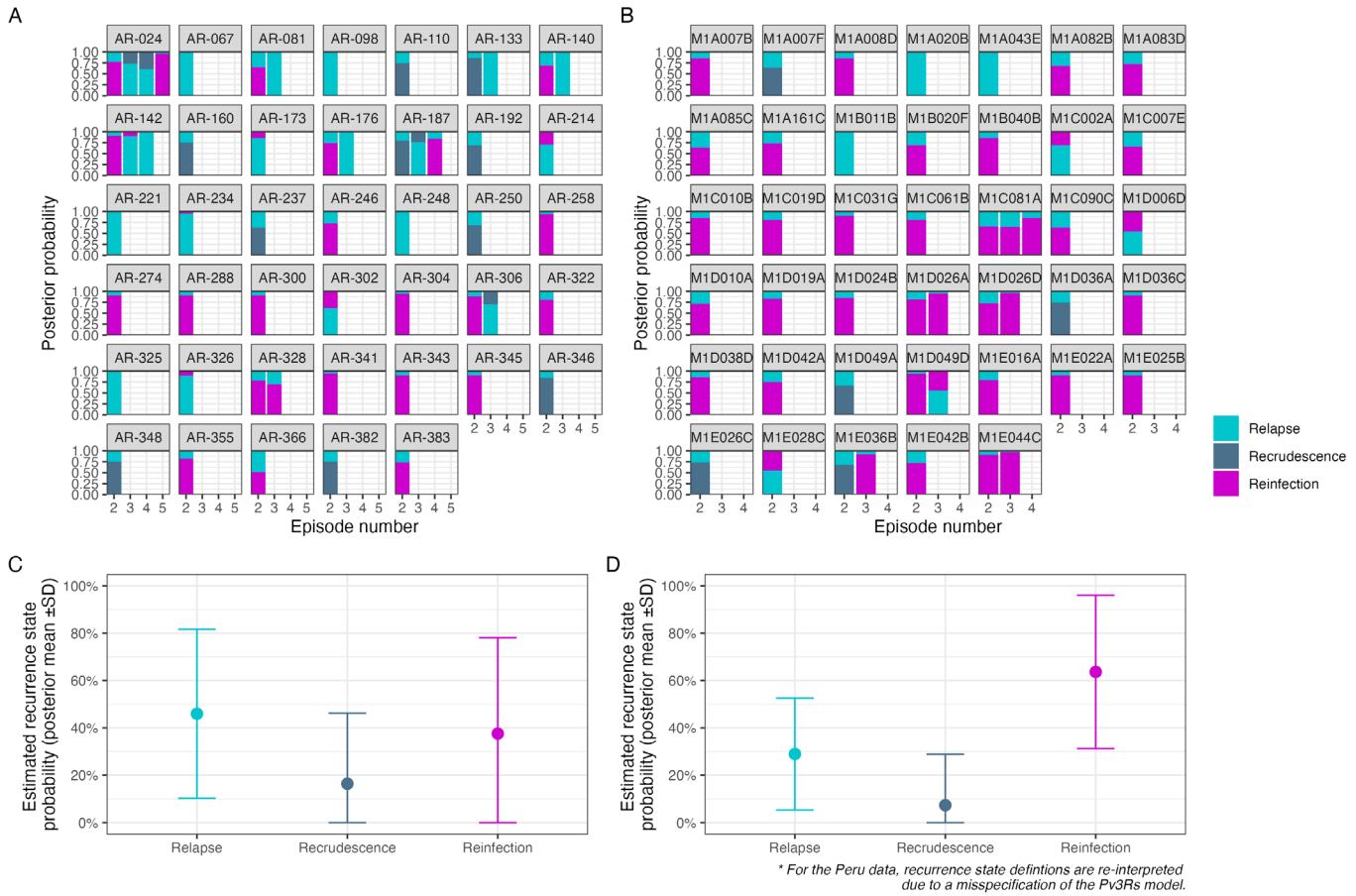

593

594 **Figure 5.** Model-based classification of recurrent *P. vivax* infections with PvAmpSeq. (A-B) Marginal posterior probabilities of relapse,
595 recrudescence, and reinfection for each recurrent infection in each participant in (A) the Solomon Islands and (B) Peru. The X-axis shows the
596 episode number; for example, considering the baseline infection as the first episode, the first recurrence would be episode 2. Note: this refers
597 to successfully genotyped episodes only (*see Supplementary Figure S12*). (C-D) Mean posterior probability estimates and standard deviation for
598 each recurrence state in (C) the Solomon Islands and (D) Peru samples. For the Peru data, due to a Pv3Rs model misspecification, recurrence
599 state definitions are re-interpreted as follows recrudescence = persistence without added relapse or reinfection; reinfection = reinfection without
600 persistence; relapse = everything else, e.g. (relapse without persistence) OR (persistence AND reinfection) etc (see Methods).

601 For Peru, after accounting for uncertainty, we found that 63.7% (SD 0.32) of participants experienced a probable
602 reinfection without persistence of a preceding infection (Pv3Rs reinfection), 7.3% (SD 0.24) experienced a probable
603 persistent infection without added relapse or reinfection (Pv3Rs recrudescence), and 29.0% experienced a probable
604 relapse (SD 0.24)(Figure 5B, 5D; see Methods for details on re-interpretation of Pv3Rs recurrence state definitions).
605 Most participants (82%, SD 0.20) experiencing more than one recurrence experienced probable reinfections without
606 persistence (Fig 5B). A sensitivity analysis using data on inter-participant episode pairs generated a mean FDR of 27.0%
607 (95% CI: 26.2–27.8 %) for the Pv3Rs model. It exceeds a mean minimum FDR of 16.2% by 10.8.

608 We explored whether the exclusion of specific markers may lead to discrepant recurrence classification. Most results,
609 particularly for Peru, did not appear to be sensitive to genotyping errors, at least not at a single marker. In 9 of 100
610 recurrences (9%), removing a single marker resulted in a non-zero recrudescence probability, with no single marker
611 driving this effect (Figure S14). Overall, we found moderate concordance between IBD estimate ranges and
612 probabilistic classification results, with the classification of high IBD recurrences also found to be either recrudescences
613 or relapses and a few reinfections. Similarly, low IBD recurrences were mostly associated with reinfections and a few
614 relapses or recrudescences, which is in line with the possibility of low-IBD heterologous relapses (Figure S15A-B). This
615 was also consistent with the microhaplotype-specific data for recurrences (Figure S16).

616 **Discussion**

617 We developed PvAmpSeq, a targeted amplicon sequencing assay that enables the characterisation of *P. vivax*
618 infections at the per-marker clonal level by targeting 11 highly polymorphic microhaplotype markers. The PvAmpSeq
619 assay amplifies field samples with >10 parasites/µL, yielding high-depth coverage but with less coverage for samples
620 with 1–10 parasites/µL. Both archived dried blood samples and red-blood-cell pellet samples were successfully
621 amplified. The high coverage per marker of PvAmpSeq allows the detection of minority clones at a frequency of >2%.
622 The PvAmpSeq microhaplotype markers comprise loci encoding surface antigens, proteins involved in reticulocyte
623 invasion, enzymes, and proteins of unknown function. As a result of immune selection acting on these loci, their high
624 diversity has made them suitable for measuring MOI and for tracking individual clones over the course of natural
625 infections within an individual.[50] Our results show that the PvAmpSeq markers provide high resolution to estimate IBD
626 in recurrent infections. The less polymorphic PvAmpSeq markers of the panel could be suitable for studying diversity
627 and structure between global regions; however, further exploration is needed to validate the assay with samples from
628 various geographical origins and in comparison to other genotyping panels (e.g.,[6,26,27,29,30]).

629 We implemented IBD to classify recurrent infections into low (<0.25 IBD), medium (0.25-0.5 IBD) and high IBD (≥0.5
630 IBD) categories compared to their baseline or preceding infection(s) and using recently developed methods,[45,46]
631 computed the probability that recurrent infections were either relapses, recrudescences, or reinfections. At the end
632 of the follow-up period, high IBD infections represented more than half of recurrent malarial episodes in the Solomon
633 Islands clinical trial, which was in line with our model estimates. After accounting for uncertainty, we found that 46%
634 of recurrences were probable relapses and 16% were probable recrudescences.

635 Our results are consistent with moderate levels of malaria transmission before the ACT-Radical clinical trial was
636 conducted in the Solomon Islands,[32] with a correspondingly high diverse parasite population. In addition, we expected
637 more moderate-to-high transmission levels with possible parasite clonal expansion in both sampled communities of
638 the Peruvian Amazon, Lupuna and Cahuide, based on previous work using microsatellite genotyping.[32,34,44] Relapsing
639 parasites with high relatedness to primary infections (high IBD) are often seen in travellers, who are likely exposed to
640 a small number of infected mosquito bites; however, this same pattern can also be seen in individuals in endemic
641 areas with a low hypnozoite load in their liver resulting in monoclonal relapses.[51–55] That relapses are involved is based
642 on the assumption that whereas some sporozoites inoculated by the mosquito become hypnozoites, others with the
643 same genotype do not.[56] Conversely, individuals in endemic areas are more likely to experience heterologous relapse
644 caused by parasites with low IBD sharing due to latent hypnozoites from previous inoculations.[51,55,57] Our data suggest
645 that the Solomon Islands cohort had a high force of infection (FOI) and likely high hypnozoite liver burden; thus,
646 polyclonal and low IBD relapses are expected to happen even in children. However, the weak population structure in
647 the Solomon Islands, suggests a frequent inbreeding environment in which the inoculation of meiotic siblings from a
648 single mosquito bite is also possible, as suggested in earlier studies.[58,59] Similarly, low IBD recurrences relative to all
649 previous infections were more frequent in the Peruvian cohort, suggesting they could encompass both relapses arising
650 from hypnozoites from previous inoculations and new infections. While the low IBD recurrences in Peru align with the
651 heterologous relapses pattern, the strong population-level connectivity makes it difficult to distinguish these from
652 reinfections. Our results showed that recurrences whose most probable state was relapse (and could be re-interpreted
653 as probable persistence and reinfection) were polyclonal and exhibited varying degrees of relatedness to the primary
654 infection, supporting previous findings in Southeast Asia and Brazil. [57,60]

655 We did not find a significant change of MOI over time, in contrast to findings reported by Noviyanti *et al*. [53], who
656 reported decreasing MOI in subsequent relapses in Indonesian soldiers returning to a malaria-free setting, which was

657 attributed to hypnozoite depletion in successive relapses. These discrepancies are likely due to our reliance on
658 endemic cohorts with individuals residing in an area with moderate-to-high transmission levels, in which both relapses
659 and new infections occur frequently, and possibly overlapping, thereby sustaining a high overall MOI. This is further
660 supported by our finding of many probable reinfections without persistence as well as evidence of relapse and/or
661 persisting infections in the Peru cohort.

662 IBD estimates (r^) correlated well with model-based classification for most recurrent infections in Peru and the
663 Solomon Islands, showing the potential application of the PvAmpSeq panel, in particular for reinfections where we
664 expect low IBD. In the case of "discordant" results, for instance where reinfections were found to also have medium
665 to high IBD, we were unable to definitively ascertain whether this was due to model misspecifications/limitations (see
666 below for discussion on model misspecifications for the Peru data) or limitations of the current PvAmpSeq panel. It is
667 likely a combination of both since the PvAmpSeq panel includes 11 microhaplotype markers and thus may not always
668 allow appropriate classification of recurrent *P. vivax* malaria infections. In some cases, more than 11 microhaplotype
669 markers may be required, depending on the circulating parasite population's genetic diversity. It is also possible that
670 recurrence classification cannot be inferred from genetic data alone. In addition, the *dcifer*-based IBD estimates
671 assume no within-host relatedness between clones, which would be inapplicable in the case of *P. vivax* relapses and
672 may impact our estimates; however, simulations by Gerlovina *et al*. showed a relatively robust estimation of IBD even
673 when this assumption is violated.[45] Our Pv3Rs sensitivity analyses where prior probabilities were varied from uniform
674 to skewed single-state priors showed that the impact on the posterior was low since population-level posterior means
675 were largely preserved, indicating robustness of Pv3Rs to prior specification. In addition, relative to its minimum, the
676 FDR for non-reinfection states (e.g. relapses and recrudescences) was small. Together these results support reporting
677 population-level (mean) posterior probabilities, where uncertainty is propagated, rather than relying on hard or
678 threshold-based individual-level assignments. The relative FDR was higher in Peru, in line with lower allelic diversity.
679 Moreover, there may be potential limitations for population-based epidemiological studies (such as that in Peru)
680 where there is no clear 'baseline' infection information given ongoing transmission and low treatment rates. A caveat
681 of the current implementation of the Pv3Rs model is that Pv3Rs was designed assuming study participants are
682 frequently and actively followed (and treated), which is appropriate for clinical trials but less so for observational
683 studies like the Peru dataset. More specifically, Pv3Rs is not designed to model persistent infections. In studies where
684 infections persist untreated (e.g., the Peruvian cohort), the state of recrudescence is ill-defined and recurrence states

685 are liable to overlap (e.g., an infectious mosquito bites a person with an untreated relapse, leading to persistent
686 relapse plus reinfection). Otherwise stated, when fit to the data from Peru, Pv3Rs is misspecified. To work around this
687 misspecification, we can reinterpret Pv3Rs's recurrence state definitions. In addition to true reinfections, the high rate
688 of reinfection that we observed in Peru could be due to people having high hypnozoite burdens at enrollment and/or
689 due to missing intermediate data (e.g. undetected recurrences/recurrences that were not successfully genotyped).
690 Another challenge for IBD-based and Pv3Rs tools is distinguishing between recrudescence and intermittent patency in
691 peripheral blood in chronic spleen-positive infections, i.e., a person might be continuously infected in the spleen,[61] but
692 parasites (all or particular clones) may only be intermittently detectable in the bloodstream; in particular, in
693 observational studies. Future work could explore refining the model-based estimates by using time-to-event models
694 to generate informative prior estimates, as was done with microsatellite data,[62] and leveraging longitudinal studies
695 with repeated sampling. Development of new models or model extensions may also be needed to robustly classify
696 recurrent infections to account for sequencing error, given the availability of many *P. vivax* amplicon sequencing
697 approaches, as well as explicitly considering the possibility of infection persistence (i.e., relaxing the assumption of
698 mutually exclusive recurrence states), but this was beyond the scope of the current study. In the context of newly
699 developed marker panels (i.e., amplicon sequencing, MIPs, and microhaplotype genotyping panels),[6,26,27,29,30] future
700 work could focus on rigorous benchmarking of these analysis tools to provide guidance for the community (e.g.,
701 PGEforge https://mrc-ide.github.io/PGEforge/).

702 Detection of microhaplotypes derived from persisting gametocytes or residual DNA in recurrent infections after ACT
703 could overestimate treatment failure rates.[63,64] Unlike *P. falciparum*, *P. vivax* gametocytes are commonly detected at
704 densities of <10% of asexual parasites, and in the absence of treatment, the duration of gametocytaemia is 3 days.[65]
705 Our approach aimed for coverage of 10,000 reads per marker per sample, ensuring high sensitivity for detecting
706 minority clones at frequencies of 0.5% within-host, i.e., 50 reads. Our sensitivity analysis showed we can confidently
707 detect microhaplotypes with ≥2% within-host frequency; thus, this approach will likely detect gametocyte
708 microhaplotypes. Interestingly, in the Solomon Islands drug-efficacy clinical trial, no recurrent infections were
709 detected earlier than 28 days post-treatment, and high IBD recurrences were more frequent in patients treated
710 without primaquine, suggestive of relapses; however, low sample sizes when stratifying by treatment arm limited us
711 from drawing definitive conclusions.

712 A limitation of our study was the number of samples included in the validation of PvAmpSeq. The original ACT-Radical
713 clinical trial involved 374 participants, of whom 307 completed follow-up,[31] but the low parasite density *P. vivax*
714 infections during follow-up limited the number of paired baseline/follow-up samples available for inclusion in
715 PvAmpSeq validation. This could also show a potential bias of PvAmpSeq to better detect new infections that usually
716 have high parasite density. After data demultiplexing and quality control, the remaining sample size per treatment
717 arm was small; thus, we could not definitively employ molecular correction to conclude the treatment efficacy
718 assessed by PvAmpSeq. Future studies should focus on enhancing the analytical sensitivity of PvAmpSeq to successfully
719 sequence samples with low parasitaemia. This methodological improvement will enable the use of larger sample sets
720 and paired samples to evaluate its application for informing on recurrences, as shown by Kleinecke *et al*.[6] The
721 sensitivity of detection of minority clones was affected by the absence of use of genetically different *P. vivax* strains
722 for mimicking mixed infections. However, the artificial mixed infection estimated that the LOD of minority clones was
723 2% when we had 10,000 reads and 1% if we had 50,000 reads. This LOD is an improvement over the 10% reported by
724 Kattenberg *et al*.,[27] while other AmpSeq panels have not yet reported this information. With these features, the
725 potential applications of PvAmpSeq we envision are i) the study of relapse biology in longitudinal studies, ii) the
726 contribution of hidden parasite biomass in spleen and bone marrow to recurrent *P. vivax* infections,[66] iii) parasite
727 diversity dynamics from human-host to mosquito vector, iv) parasite population diversity within mosquitoes collected
728 in cross-sectional studies.

729 Likewise, in the Peruvian cohort, some intermediate low-density/submicroscopic infections could have been missed;
730 thus, some of the recurrent infections might not reflect the real infection dynamics in this population. The DNA quality
731 from low parasite density samples represented a challenge for PvAmpSeq, as observed in samples with 1–10
732 parasites/µL that were discarded due to low coverage (38% of the Solomon Islands samples and 49% of the Peruvian
733 samples). Selective Whole Genome Amplification (sWGA) has been demonstrated to improve sample coverage in very
734 low *Plasmodium* density samples for AmpSeq or WGS methods.[16–18,27,67] However, this type of treatment to low-density
735 samples could incur amplification biases of the most dominant clone, increase the error rate and raise costs, making
736 it less applicable in low-resources settings.[17,18] Other factors may also influence the applicability of PvAmpSeq, like
737 daily fluctuations in clone densities within infection, which may impede robust longitudinal tracking of clones,
738 particularly minor clones. Although we tested 6 PvAmpSeq markers in paired dried-blood spot and red-blood-cell pellet
739 samples, we were not able to evaluate the complete panel of markers in this sample subset due to limited DNA

740 quantities. Nevertheless, we found that PvAmpSeq performed well on both sample types, albeit with better recovery
741 of the number of microhaplotype variants for some of the markers. PvAmpSeq detected more polyclonal infections
742 than microsatellite genotyping in a small subset of Peruvian samples; however, future studies should include larger
743 sample sizes to evaluate the applicability of PvAmpSeq to quantify polyclonal infections in other settings.

744 AmpSeq has been proposed as a new gold standard for analysing malaria drug clinical trials.[3,12] For *P. falciparum*, five
745 AmpSeq markers have been validated to discern between recrudescences and reinfections.[5] Regardless of the level of
746 endemicity and the cut-off of detection for minority clones (0.1–2%), simulation studies showed that the use of 3 to 5
747 polymorphic markers was sufficient to classify *P. falciparum* recurrent infections as recrudescences or reinfections.[12]
748 In *P. vivax* infections, genotyping of highly related sibling progeny present in a relapse may not always be possible
749 when using a limited number of markers. However, this challenge can be overcome by using polymorphic markers,
750 such as those in the present panel, which offer a theoretical range of 2^7 to 2^6 (64-128) possible combinations per locus,
751 based on the median SNP density, providing a high multi-locus resolution. WGS analysis has demonstrated that
752 relapses can be meiotic siblings resulting from the same recombination event, contrary to what microsatellite
753 genotyping classified as identical or clonal.[68] Recent *P. vivax* wide-genome panels of Ampseq markers could potentially
754 address this question;[6,26,27,29] however, increasing marker coverage to 10,000 reads would represent higher costs for
755 laboratories in low-resource settings. Using PvAmpSeq data, we estimated IBD and calculated posterior probability
756 estimates of recurrences being relapses, recrudescences or reinfections by using the information from 11
757 microhaplotype markers. We found that this classification using both methods was largely concordant in samples from
758 both the Solomon Islands clinical trial and the Peruvian community cohort. Nevertheless, simulation studies and/or
759 studies conducted in other epidemiological contexts could inform whether the number of PvAmpSeq markers included
760 in this study would be sufficient for classifying recurrent infections in clinical trials executed in settings with higher
761 endemicity levels of *P. vivax* than in this study.

762 Despite the advancements offered by high-coverage panels like PvAmpSeq, a major challenge in distinguishing
763 relapses from reinfections remains the inherent limitation of current analytical classification tools (e.g., Pv3Rs). These
764 methods rely on specific assumptions; for example, Pv3Rs assumes recurrence states are either relapse, recrudescence
765 or reinfection where recurrence states are mutually exclusive, assumes no genotyping errors, and does not model
766 persistent infections. For instance, a reinfection may be mistakenly classified as a relapse if the recurrence parasite
767 shows high IBD with the previous infection, as might happen in household transmissions. Conversely, a relapse will

768 have a high reinfection probability if the relapsing parasite exhibits low IBD due to diversity in the hypnozoite reservoir.
769 The Pv3Rs model considers the possibility of residual relapse even if the genetic data are consistent with reinfection
770 (i.e., low IBD), but assumes that recurrence states are mutually exclusive, which may limit applicability in certain
771 settings where recurrence states are liable to overlap. Furthermore, current genotyping approaches are constrained
772 by technical limitations, as they are typically restricted to using DNA derived from blood-stage infections. This
773 approach provides an incomplete picture, as the genetic diversity of the dormant hypnozoite reservoir (the "ground
774 truth" for relapse origin) cannot be directly determined. Given these classification constraints, we adopted a strategy
775 of presenting results from both IBD-based classification methods and model-based classification methods, the
776 integration of which provides a more robust and suitable approach for the analysis of *P. vivax* recurrence patterns.

777 In conclusion, here we present a new framework to classify *P. vivax* recurrent infections using PvAmpSeq
778 microhaplotype data for molecular correction in drug clinical trials and for studying *P. vivax* relapse biology in
779 longitudinal cohorts, and demonstrate its potential using state-of-the-art analysis methods. We anticipate that this
780 tool can be applied in a wide range of epidemiological studies and clinical trials to fill a pressing need in *P. vivax*
781 genomic epidemiology to better understand relapse epidemiology and support the robust evaluation of clinical
782 efficacy trials.

783

784 References

785 1. World Health Organisation (2024). World malaria report 2024.

786 2. Robinson, L.J., Wampfler, R., Betuela, I., Karl, S., White, M.T., Li Wai Suen, C.S., Hofmann, N.E., Kinboro, B.,
787 Waltmann, A., Brewster, J., *et al.* (2015). Strategies for understanding and reducing the Plasmodium vivax and
788 Plasmodium ovale hypnozoite reservoir in Papua New Guinean children: a randomised placebo-controlled trial
789 and mathematical model. PLoS Med. *12*, e1001891.

790 3. World Health Organisation (2021). Informal consultation on methodology to distinguish reinfection from
791 recrudescence in high malaria transmission areas.

792 4. World Health Organisation (2008). Methods and techniques for clinical trials on antimalarial drug efficacy:
793 genotyping to identify parasite populations.

794 5. Gruenberg, M., Lerch, A., Beck, H.P., and Felger, I. (2019). Amplicon deep sequencing improves Plasmodium
795 falciparum genotyping in clinical trials of antimalarial drugs. Sci. Rep. *9*, 17790.

796 6. Kleinecke, M., Sutanto, E., Rumaseb, A., Hoon, K.S., Trimarsanto, H., Osborne, A., Manrique, P., Peters, T., Hawkes,
797 D., Benavente, E.D., *et al.* (2025). Microhaplotype deep sequencing assays to capture Plasmodium vivax infection
798 lineages. Nat. Commun. *16*, 7192.

7. Lerch, A., Koepfli, C., Hofmann, N.E., Messerli, C., Wilcox, S., Kattenberg, J.H., Betuela, I., O'Connor, L., Mueller, I., and Felger, I. (2017). Development of amplicon deep sequencing markers and data analysis pipeline for genotyping multi-clonal malaria infections. BMC Genomics *18*, 864.

8. Ruybal-Pesántez, S., McCann, K., Vibin, J., Siegel, S., Auburn, S., and Barry, A.E. (2024). Molecular markers for malaria genetic epidemiology: progress and pitfalls. Trends Parasitol. *40*, 147–163.

9. Lerch, A., Koepfli, C., Hofmann, N.E., Kattenberg, J.H., Rosanas-Urgell, A., Betuela, I., Mueller, I., and Felger, I. (2019). Longitudinal tracking and quantification of individual Plasmodium falciparum clones in complex infections. Sci. Rep. *9*, 3333.

10. Lin, J.T., Hathaway, N.J., Saunders, D.L., Lon, C., Balasubramanian, S., Kharabora, O., Gosi, P., Sriwichai, S., Kartchner, L., Chuor, C.M., *et al.* (2015). Using Amplicon Deep Sequencing to Detect Genetic Signatures of Plasmodium vivax Relapse. J. Infect. Dis. *212*, 999–1008.

11. Wamae, K., Ndwiga, L., Kharabora, O., Kimenyi, K., Osoti, V., De Laurent, Z.R., Wambua, J., Musyoki, J., Ngetsa, C., Kalume, P., *et al.* (2022). Targeted amplicon deep sequencing of ama1 and mdr1 to track within-host P. falciparum diversity throughout treatment in a clinical drug trial [version 2; peer review: 1 approved, 1 approved with reservations]. Wellcome Open Res. *7:95*. 10.12688/wellcomeopenres.17736.2.

12. Jones, S., Kay, K., Hodel, E.M., Gruenberg, M., Lerch, A., Felger, I., and Hastings, I. (2021). Should Deep-Sequenced Amplicons Become the New Gold Standard for Analyzing Malaria Drug Clinical Trials? Antimicrob. Agents Chemother. *65*, e0043721.

13. He, X., Zhong, D., Zou, C., Pi, L., Zhao, L., Qin, Y., Pan, M., Wang, S., Zeng, W., Xiang, Z., *et al.* (2021). Unraveling the Complexity of Imported Malaria Infections by Amplicon Deep Sequencing. Front. Cell. Infect. Microbiol. *11*, 725859.

14. Wamae, K., Kimenyi, K.M., Osoti, V., de Laurent, Z.R., Ndwiga, L., Kharabora, O., Hathaway, N.J., Bailey, J.A., Juliano, J.J., Bejon, P., *et al.* (2022). Amplicon Sequencing as a Potential Surveillance Tool for Complexity of Infection and Drug Resistance Markers in Plasmodium falciparum Asymptomatic Infections. J. Infect. Dis. *226*, 920–927.

15. Holzschuh, A., Lerch, A., Fakih, B.S., Aliy, S.M., Ali, M.H., Ali, M.A., Bruzzese, D.J., Yukich, J., Hetzel, M.W., and Koepfli, C. (2024). Using a mobile nanopore sequencing lab for end-to-end genomic surveillance of Plasmodium falciparum: A feasibility study. PLOS Glob. Public Health *4*, e0002743.

16. LaVerriere, E., Schwabl, P., Carrasquilla, M., Taylor, A.R., Johnson, Z.M., Shieh, M., Panchal, R., Straub, T.J., Kuzma, R., Watson, S., *et al.* (2022). Design and implementation of multiplexed amplicon sequencing panels to serve genomic epidemiology of infectious disease: A malaria case study. Mol. Ecol. Resour. *22*, 2285–2303.

17. Kattenberg, J.H., Van Dijk, N.J., Fernandez-Minope, C.A., Guetens, P., Mutsaers, M., Gamboa, D., and Rosanas-Urgell, A. (2023). Molecular Surveillance of Malaria Using the PF AmpliSeq Custom Assay for Plasmodium falciparum Parasites from Dried Blood Spot DNA Isolates from Peru. Bio Protoc. *13*, e4621.

18. Kattenberg, J.H., Fernandez-Minope, C., van Dijk, N.J., Llacsahuanga Allcca, L., Guetens, P., Valdivia, H.O., Van Geertruyden, J.P., Rovira-Vallbona, E., Monsieurs, P., Delgado-Ratto, C., *et al.* (2023). Malaria Molecular Surveillance in the Peruvian Amazon with a Novel Highly Multiplexed Plasmodium falciparum AmpliSeq Assay. Microbiol. Spectr. *11*, e0096022.

19. Talundzic, E., Ravishankar, S., Kelley, J., Patel, D., Plucinski, M., Schmedes, S., Ljolje, D., Clemons, B., Madison-Antenucci, S., Arguin, P.M., *et al.* (2018). Next-generation sequencing and bioinformatics protocol for malaria drug resistance marker surveillance. Antimicrob. Agents Chemother. *62*. 10.1128/AAC.02474-17.

20. Huwe, T., Kibria, M.G., Johora, F.T., Phru, C.S., Jahan, N., Hossain, M.S., Khan, W.A., Price, R.N., Ley, B., Alam, M.S., *et al.* (2022). Heterogeneity in prevalence of subclinical Plasmodium falciparum and Plasmodium vivax infections but no parasite genomic clustering in the Chittagong Hill Tracts, Bangladesh. Malar. J. *21*, 218.

21. Wei, X., Malla, P., Wang, Z., Yang, Z., Cao, Y., Wang, C., and Cui, L. (2024). Genetic diversity of Plasmodium vivax population in northeast Myanmar assessed by amplicon sequencing of PvMSP1 and PvMSP3α. Acta Trop. *260*, 107461.

22. Tapaopong, P., da Silva, G., Holzschuh, A., Rungsarityotin, W., Suansomjit, C., Pumchuea, K., Manopwisedjaroen, K., Khamsiriwatchara, A., Khuntong, P., Cui, L., *et al.* (2025). Molecular epidemiology and genetic diversity of disappearing Plasmodium vivax in southern Thailand. Sci. Rep. *15*, 2620.

23. Reda, A.G., Huwe, T., Koepfli, C., Assefa, A., Tessema, S.K., Messele, A., Golassa, L., and Mamo, H. (2023). Amplicon deep sequencing of five highly polymorphic markers of Plasmodium falciparum reveals high parasite genetic diversity and moderate population structure in Ethiopia. Malar. J. *22*, 376.

24. Tapaopong, P., da Silva, G., Chainarin, S., Suansomjit, C., Manopwisedjaroen, K., Cui, L., Koepfli, C., Sattabongkot, J., and Nguitragool, W. (2023). Genetic diversity and molecular evolution of Plasmodium vivax Duffy Binding Protein and Merozoite Surface Protein-1 in northwestern Thailand. Infect. Genet. Evol. *113*, 105467.

25. Holzschuh, A., Lerch, A., Gerlovina, I., Fakih, B.S., Al-Mafazy, A.-W.H., Reaves, E.J., Ali, A., Abbas, F., Ali, M.H., Ali, M.A., *et al.* (2023). Multiplexed ddPCR-amplicon sequencing reveals isolated Plasmodium falciparum populations amenable to local elimination in Zanzibar, Tanzania. Nat. Commun. *14*, 3699.

26. Siegel, S.V., Trimarsanto, H., Amato, R., Murie, K., Taylor, A.R., Sutanto, E., Kleinecke, M., Whitton, G., Watson, J.A., Imwong, M., *et al.* (2024). Lineage-informative microhaplotypes for recurrence classification and spatio-temporal surveillance of Plasmodium vivax malaria parasites. Nat. Commun. *15*, 6757.

27. Kattenberg, J.H., Nguyen, H.V., Nguyen, H.L., Sauve, E., Nguyen, N.T.H., Chopo-Pizarro, A., Trimarsanto, H., Monsieurs, P., Guetens, P., Nguyen, X.X., *et al.* (2022). Novel highly-multiplexed AmpliSeq targeted assay for Plasmodium vivax genetic surveillance use cases at multiple geographical scales. Front. Cell. Infect. Microbiol. *12*, 953187.

28. Kattenberg, J.H., Cabrera-Sosa, L., Figueroa-Ildefonso, E., Mutsaers, M., Monsieurs, P., Guetens, P., Infante, B., Delgado-Ratto, C., Gamboa, D., and Rosanas-Urgell, A. (2024). Plasmodium vivax genomic surveillance in the Peruvian Amazon with Pv AmpliSeq assay. PLoS Negl. Trop. Dis. *18*, e0011879.

29. Popkin-Hall, Z.R., Niaré, K., Crudale, R., Simkin, A., Fola, A.A., Sanchez, J.F., Pannebaker, D.L., Giesbrecht, D.J., Kim, I.E., Jr, Aydemir, Ö., *et al.* (2024). High-throughput genotyping of Plasmodium vivax in the Peruvian Amazon via molecular inversion probes. Nat. Commun. *15*, 10219.

30. Hubbard, A., Solares, E., Bradley, L., Jeang, B., Yewhalaw, D., Janies, D., Lo, E., Yan, G., and Hemming-Schroeder, E. (2025). PvGAP: Development of a globally-applicable, highly-multiplexed microhaplotype amplicon panel for Plasmodium vivax. medRxiv. 10.1101/2025.04.30.25326751.

31. James, R., Obadia, T., Wini, L., Bobogare, A., Charnaud, S., Ruybal-Pesántez, S., Bourke, C., Munro, J.E., Moore, B.R., Page-Sharp, M., *et al.* (2025). Efficacy of low-dose primaquine plus artemether-lumefantrine or dihydroartemisinin-piperaquine for radical cure of Plasmodium vivax in the Solomon Islands: a randomised clinical trial. Front. Malar. *3*. 10.3389/fmala.2025.1604498.

32. Rosado, J., White, M.T., Longley, R.J., Lacerda, M., Monteiro, W., Brewster, J., Sattabongkot, J., Guzman-Guzman, M., Llanos-Cuentas, A., Vinetz, J.M., *et al.* (2021). Heterogeneity in response to serological exposure markers of recent Plasmodium vivax infections in contrasting epidemiological contexts. PLoS Negl. Trop. Dis. *15*, e0009165.

33. Han, J., Munro, J.E., and Bahlo, M. (2023). AmpSeqR: an R package for amplicon deep sequencing data analysis [version 1; peer review: awaiting peer review]. F1000Res. *12*. 10.12688/f1000research.129581.1.

883 34. Rosas-Aguirre, A., Guzman-Guzman, M., Chuquiyauri, R., Moreno, M., Manrique, P., Ramirez, R., Carrasco-
884 Escobar, G., Rodriguez, H., Speybroeck, N., Conn, J.E., *et al.* (2021). Temporal and Microspatial Heterogeneity in
885 Transmission Dynamics of Coendemic Plasmodium vivax and Plasmodium falciparum in Two Rural Cohort
886 Populations in the Peruvian Amazon. J. Infect. Dis. *223*, 1466–1477.

887 35. Carrasco-Escobar, G., Miranda-Alban, J., Fernandez-Minope, C., Brouwer, K.C., Torres, K., Calderon, M., Gamboa,
888 D., Llanos-Cuentas, A., and Vinetz, J.M. (2017). High prevalence of very-low Plasmodium falciparum and
889 Plasmodium vivax parasitaemia carriers in the Peruvian Amazon: insights into local and occupational mobility-
890 related transmission. Malar. J. *16*, 415.

891 36. Mangold, K.A., Manson, R.U., Koay, E.S., Stephens, L., Regner, M., Thomson, R.B., Jr, Peterson, L.R., and Kaul, K.L.
892 (2005). Real-time PCR for detection and identification of Plasmodium spp. J. Clin. Microbiol. *43*, 2435–2440.

893 37. Rosanas-Urgell, A., Mueller, D., Betuela, I., Barnadas, C., Iga, J., Zimmerman, P.A., del Portillo, H.A., Siba, P.,
894 Mueller, I., and Felger, I. (2010). Comparison of diagnostic methods for the detection and quantification of the
895 four sympatric Plasmodium species in field samples from Papua New Guinea. Malar. J. *9*, 361.

896 38. Pearson, R.D., Amato, R., Auburn, S., Miotto, O., Almagro-Garcia, J., Amaratunga, C., Suon, S., Mao, S., Noviyanti,
897 R., Trimarsanto, H., *et al.* (2016). Genomic analysis of local variation and recent evolution in Plasmodium vivax.
898 Nat. Genet. *48*, 959–964.

899 39. Li, H., Handsaker, B., Wysoker, A., Fennell, T., Ruan, J., Homer, N., Marth, G., Abecasis, G., Durbin, R., and Genome
900 Project Data Processing, Subgroup (2009). The Sequence Alignment/Map format and SAMtools. Bioinformatics
901 *25*, 2078–2079.

902 40. Untergasser, A., Cutcutache, I., Koressaar, T., Ye, J., Faircloth, B.C., Remm, M., and Rozen, S.G. (2012). Primer3--
903 new capabilities and interfaces. Nucleic Acids Res. *40*, e115.

904 41. Pagès, H., Aboyoun, P., Gentleman, R., and DebRoy, S. (2024). Biostrings: Efficient manipulation of biological
905 strings. R package version 2.72.1.

906 42. Morgan, M., Anders, S., Lawrence, M., Aboyoun, P., Pages, H., and Gentleman, R. (2009). ShortRead: a
907 bioconductor package for input, quality assessment and exploration of high-throughput sequence data.
908 Bioinformatics *25*, 2607–2608.

909 43. Havryliuk, T., and Ferreira, M.U. (2009). A closer look at multiple-clone Plasmodium vivax infections: detection
910 methods, prevalence and consequences. Mem. Inst. Oswaldo Cruz *104*, 67–73.

911 44. Manrique, P., Miranda-Alban, J., Alarcon-Baldeon, J., Ramirez, R., Carrasco-Escobar, G., Herrera, H., Guzman-
912 Guzman, M., Rosas-Aguirre, A., Llanos-Cuentas, A., Vinetz, J.M., *et al.* (2019). Microsatellite analysis reveals
913 connectivity among geographically distant transmission zones of Plasmodium vivax in the Peruvian Amazon: A
914 critical barrier to regional malaria elimination. PLoS Negl. Trop. Dis. *13*, e0007876.

915 45. Gerlovina, I., Gerlovin, B., Rodriguez-Barraquer, I., and Greenhouse, B. (2022). Dcifer: an IBD-based method to
916 calculate genetic distance between polyclonal infections. Genetics *222*. 10.1093/genetics/iyac126.

917 46. Foo, Y.S., White, M.T., and Taylor, A.R. (2026). Pv3Rs: Plasmodium vivax relapse, recrudescence, and reinfection
918 statistical genetic inference. Bioinformatics *42*. 10.1093/bioinformatics/btaf643.

919 47. White, N.J. (2011). Determinants of relapse periodicity in Plasmodium vivax malaria. Malar. J. *10*, 297.

920 48. Mideo, N., Kennedy, D.A., Carlton, J.M., Bailey, J.A., Juliano, J.J., and Read, A.F. (2013). Ahead of the curve: next
921 generation estimators of drug resistance in malaria infections. Trends Parasitol. *29*, 321–328.

922 49. White, N.J. (2021). Anti-malarial drug effects on parasite dynamics in vivax malaria. Malar. J. *20*, 161.

923 50. Barry, A.E., Waltmann, A., Koepfli, C., Barnadas, C., and Mueller, I. (2015). Uncovering the transmission dynamics
924 of Plasmodium vivax using population genetics. Pathog. Glob. Health *109*, 142–152.

925 51. Imwong, M., Boel, M.E., Pagornrat, W., Pimanpanarak, M., McGready, R., Day, N.P., Nosten, F., and White, N.J.
926 (2012). The first Plasmodium vivax relapses of life are usually genetically homologous. J. Infect. Dis. *205*, 680–
927 683.

928 52. Chen, N., Auliff, A., Rieckmann, K., Gatton, M., and Cheng, Q. (2007). Relapses of Plasmodium vivax infection
929 result from clonal hypnozoites activated at predetermined intervals. J. Infect. Dis. *195*, 934–941.

930 53. Noviyanti, R., Carey-Ewend, K., Trianty, L., Parobek, C., Puspitasari, A.M., Balasubramanian, S., Park, Z., Hathaway,
931 N., Utami, R.A.S., Soebianto, S., *et al.* (2022). Hypnozoite depletion in successive Plasmodium vivax relapses. PLoS
932 Negl. Trop. Dis. *16*, e0010648.

933 54. Delgado-Ratto, C., Soto-Calle, V.E., Van den Eede, P., Gamboa, D., Rosas, A., Abatih, E.N., Rodriguez Ferrucci, H.,
934 Llanos-Cuentas, A., Van Geertruyden, J.-P., Erhart, A., *et al.* (2014). Population structure and spatio-temporal
935 transmission dynamics of Plasmodium vivax after radical cure treatment in a rural village of the Peruvian Amazon.
936 Malar. J. *13*, 8.

937 55. Cowell, A.N., Valdivia, H.O., Bishop, D.K., and Winzeler, E.A. (2018). Exploration of Plasmodium vivax transmission
938 dynamics and recurrent infections in the Peruvian Amazon using whole genome sequencing. Genome Med. *10*,
939 52.

940 56. Markus, M.B. (2012). Source of homologous parasites in recurrent Plasmodium vivax malaria. J. Infect. Dis. *206*,
941 622–623.

942 57. de Araujo, F.C., de Rezende, A.M., Fontes, C.J., Carvalho, L.H., and Alves de Brito, C.F. (2012). Multiple-clone
943 activation of hypnozoites is the leading cause of relapse in Plasmodium vivax infection. PLoS One *7*, e49871.

944 58. Koepfli, C., Timinao, L., Antao, T., Barry, A.E., Siba, P., Mueller, I., and Felger, I. (2013). A large Plasmodium vivax
945 reservoir and little population structure in the South Pacific. PLoS One *8*, e66041.

946 59. Gray, K.-A., Dowd, S., Bain, L., Bobogare, A., Wini, L., Shanks, G.D., and Cheng, Q. (2013). Population genetics of
947 Plasmodium falciparum and Plasmodium vivax and asymptomatic malaria in Temotu Province, Solomon Islands.
948 Malar. J. *12*, 429.

949 60. Popovici, J., Friedrich, L.R., Kim, S., Bin, S., Run, V., Lek, D., Cannon, M.V., Menard, D., and Serre, D. (2018).
950 Genomic Analyses Reveal the Common Occurrence and Complexity of Plasmodium vivax Relapses in Cambodia.
951 MBio *9*. 10.1128/mBio.01888-17.

952 61. Kho, S., Qotrunnada, L., Leonardo, L., Andries, B., Wardani, P.A.I., Fricot, A., Henry, B., Hardy, D., Margyaningsih,
953 N.I., Apriyanti, D., *et al.* (2021). Hidden biomass of intact malaria parasites in the human spleen. N. Engl. J. Med.
954 *384*, 2067–2069.

955 62. Taylor, A.R., Watson, J.A., Chu, C.S., Puaprasert, K., Duanguppama, J., Day, N.P.J., Nosten, F., Neafsey, D.E.,
956 Buckee, C.O., Imwong, M., *et al.* (2019). Resolving the cause of recurrent Plasmodium vivax malaria
957 probabilistically. Nat. Commun. *10*, 5595.

958 63. Hasugian, A.R., Purba, H.L., Kenangalem, E., Wuwung, R.M., Ebsworth, E.P., Maristela, R., Penttinen, P.M., Laihad,
959 F., Anstey, N.M., Tjitra, E., *et al.* (2007). Dihydroartemisinin-piperaquine versus artesunate-amodiaquine: superior
960 efficacy and posttreatment prophylaxis against multidrug-resistant Plasmodium falciparum and Plasmodium
961 vivax malaria. Clin. Infect. Dis. *44*, 1067–1074.

962 64. Pukrittayakamee, S., Imwong, M., Singhasivanon, P., Stepniewska, K., Day, N.J., and White, N.J. (2008). Effects of
963 different antimalarial drugs on gametocyte carriage in P. vivax malaria. Am. J. Trop. Med. Hyg. *79*, 378–384.

964 65. Bousema, T., and Drakeley, C. (2011). Epidemiology and infectivity of Plasmodium falciparum and Plasmodium
965 vivax gametocytes in relation to malaria control and elimination. Clin. Microbiol. Rev. *24*, 377–410.

966 66. Markus, M.B. (2017). Malaria eradication and the hidden parasite reservoir. Trends Parasitol. *33*, 492–495.

967 67. Oyola, S.O., Ariani, C.V., Hamilton, W.L., Kekre, M., Amenga-Etego, L.N., Ghansah, A., Rutledge, G.G., Redmond,
968 S., Manske, M., Jyothi, D., *et al.* (2016). Whole genome sequencing of Plasmodium falciparum from dried blood
969 spots using selective whole genome amplification. Malar. J. *15*, 597.

970 68. Bright, A.T., Manary, M.J., Tewhey, R., Arango, E.M., Wang, T., Schork, N.J., Yanow, S.K., and Winzeler, E.A. (2014).
971 A high resolution case study of a patient with recurrent Plasmodium vivax infections shows that relapses were
972 caused by meiotic siblings. PLoS Negl. Trop. Dis. *8*, e2882.

973 # Key resources table

Reagent or Resource	Source	Identifier
Bacterial and Virus Strains		
Enterobacteria phage PhiX control v3	Illumina	Cat# **FC-110-3001**
Chemicals, Peptides, and Recombinant Proteins		
GoTaq® Probe qPCR Master Mix	Promega	Cat# **A6102**
Quant-iT PicoGreen® dsDNA kit	Thermo Fisher Scientific	Cat# **P7589**
Critical Commercial Assays		
Favorprep 96-well genomic DNA kit	Favorgen	Cat# **FADWE 96004**
E.Z.N.A. Blood DNA Mini Kit	Omega Bio-tek, Inc.	Cat# **D3392-02**
QIAGEN MinElute 96 UF PCR Purification Kit	QIAGEN	Cat# **28053**
NucleoMag® NGS beads	Macherey-Nagel	Cat# **744970. 50**
MiSeq reagent kit v3 (600 cycles; 2 × 300 bp)	Illumina	N/A
Oligonucleotides		
PvAmpSeq Primers/Probes (Primary, Secondary, Index)	Eurofins	Sequences provided in https://doi.org/10.5281/zenodo.17474689
Duplex TaqMan qPCR Primers/Probes (Pv and Pf 18s rRNA)	Eurofins	Sequences listed in reference 36
Software and Algorithms		
R 4.1.0	The R Foundation	RRID: SCR_001905
AmpSeqR version 0.1	Bahlolab (via GitHub)	https://github.com/bahlolab/AmpSeqR
dcifer R package	Gerlovina I. *et al*. 2022	https://eppicenter.github.io/dcifer/
Pv3Rs R package	Taylor A.R. *et al.* 2022	https://github.com/aimeertaylor/Pv3Rs
Primer3	Untergasser, A. *et al.* 2012	RRID: SCR_003139
Biostrings R package	Pagès, H. *et al.* 2024	N/A (Standard R package)
ShortRead R package	Morgan, M. *et al*. 2009	N/A (Standard R package)

GATK V4	Broad Institute	RRID: SCR_001876
Other		
QuantStudio TM 5 Real-Time PCR system	Applied Biosystems	Cat# **A28140**
Agilent D5000 ScreenTape System	Agilent Technologies	Cat# **G2991AA**
Illumina MiSeq platform	Illumina	N/A
PvAmpSeq Genotyping SOP	Zenodo	https://doi.org/10.5281/zenodo.17474689

Acknowledgments

We thank the participants who anonymously agreed to participate in the ACT-Radical clinical trial and the ICEMR study. We acknowledge the field teams that contributed to sample collection in the Solomon Islands and Peru, and Soazic Gardais for logistical support at Institut Pasteur, Paris. We thank Leanne Robinson for provision of the control DNA samples. We thank Prof Miles Markus for his input and suggestions on our manuscript. This work was also made possible through the Victorian State Government Operational Infrastructure Support and Australian Government National Health and Medical Research Council Independent Research Institute Infrastructure Support Scheme. The study was supported by a grant from the Bill and Melinda Gates Foundation (funding grant ID number: OPP1151132). IM was supported by an Australian National Health and Medical Research Council (NHMRC) Investigator Grant (#2016726). MB was supported by an Australian NHMRC Investigator Grant (GNT1195236). The Peruvian cohort was part of the Amazonian International Center of Excellence in Malaria Research that received funding through the Cooperative Agreement U19AI089681 from the US Public Health Service, National Institutes of Health/National Institute of Allergy and Infectious Diseases, USA to JMV, and from a FOGARTY global infectious disease training grant (2D43TW007120-11A1, NIH-USA to JMV). ART is funded by the European Union (project number 101110393). Views and opinions expressed are however those of the author only and do not necessarily reflect those of the European Union or European Research Executive Agency (REA). Neither the European Union nor the granting authority can be held responsible for them. This work was supported by the French government's "Integrative Biology of Emerging Infectious Diseases" (Investissement d'Avenir grant ANR-10-LABX-62-IBEID) and INCEPTION (Investissement d'Avenir grant ANR-16-CONV-0005) programs to MW. JR postdoctoral fellowship was funded by Institut de Recherche pour le Développement. SR-P acknowledges funding from the MRC Centre for Global Infectious Disease Analysis (reference MR/X020258/1), funded by the UK Medical Research Council (MRC). This UK-funded award is carried out in the frame of the Global Health EDCTP3 Joint Undertaking.

Author's contributions

JR, IM, and SRP designed the study. JR and SRP designed PvAmpSeq protocols. JR, ZT, KS, JB and CB did the genotyping. JH, JM, and MB developed AmpSeqR and preprocessed sequencing data, with contributions from JR, SRP, TO and CB. JR, TO, ART and SRP analysed the data and performed statistical analyses. JMV, MTW, MB, DG, and IM provided administrative and logistical support. JR and SRP wrote the first draft of the manuscript. All authors had full access to all the data. All authors contributed to the manuscript's writing.

Declaration of interest

The authors declare no competing interests.

Supplemental information

Document S1. Figures S1–S16

Document S2. Table S1–S9

Text S1. Excel file containing additional data on PvAmpSeq markers, too large to fit in a PDF.

Text S2. Data of IBD estimates in Solomon Islands cohort.

Text S3. Data of IBD estimates in the Peruvian cohort.

Table 1. Epidemiological characteristics of participants and description of their infections

Participant characteristics	**Solomon Islands** **n = 77**	**Peru** **n = 93**
Age, median [IQR]	10.1 [7.42– 14.4]	36.7 [18.0– 51.5]
Sex, number female (%)	32 (41.6%)	51 (54.8%)
Treatment administered	Artemether-lumefantrine (n = 21), artemether-lumefantrine + primaquine (n = 25), dihydroartemisinin-piperaquine + primaquine (n = 31)	Chloroquine-primaquine (n=1)
Infection characteristics	**n = 135**	**n = 140**
Parasite density, median [IQR]		
Baseline	416 parasites/µL [81.7– 793][a]	341 parasites/µL [40.6– 8560][b]
Follow-up	151 parasites/µL [18.1– 978]	337 parasites/µL [77.6– 1470]
Febrile, number (%)		
Baseline	38/77 (49.4%)[c]	7/93 (7.5%)[d]
Follow-up	11/58 (19.0%)	2/47 (4.3%)

a Statistical difference between baseline and follow-up assessed by a two-sided Mann-Whitney test, $p = 0.2515$.
b Statistical difference between baseline and follow-up assessed by a two-sided Mann-Whitney test, $p = 0.7541$.
c Statistical difference between baseline and follow-up assessed by a two-sided Fisher's exact test, $p = 0.0003$.
d Statistical difference between baseline and follow-up assessed by a two-sided Fisher's exact test, $p = 0.7178$.